

HARP Collaboration

Measurements of forward proton production with incident protons and charged pions on nuclear targets at the CERN Proton Synchrotron.

Measurements of the double-differential proton production cross-section $d^2\sigma/dpd\Omega$ in the range of momentum $0.5 \text{ GeV}/c \leq p < 8.0 \text{ GeV}/c$ and angle $0.05 \text{ rad} \leq \theta < 0.25 \text{ rad}$ in collisions of charged pions and protons on beryllium, carbon, aluminium, copper, tin, tantalum and lead are presented. The data were taken with the large acceptance HARP detector in the T9 beam line of the CERN Proton Synchrotron. Incident particles were identified by an elaborate system of beam detectors and impinged on a target of 5% of a nuclear interaction length. The tracking and identification of the produced particles was performed using the forward spectrometer of the HARP experiment. Results are obtained for the double-differential cross-sections mainly at four incident beam momenta (3 GeV/c, 5 GeV/c, 8 GeV/c and 12 GeV/c). Measurements are compared with predictions of the GEANT4 and MARS Monte Carlo generators.

M. Apollonio,^{1, a} A. Artamonov,^{2, b} A. Bagulya,³ G. Barr,⁴ A. Blondel,⁵ F. Bobisut^(**),⁶
M. Bogomilov,⁷ M. Bonesini,^{8, c} C. Booth,⁹ S. Borghi,^{5, d} S. Bunyatov,¹⁰ J. Burguet–Castell,¹¹
M.G. Catanesi,¹² A. Cervera–Villanueva,¹¹ P. Chimenti,¹ L. Coney,^{· e} E. Di Capua,¹³ U. Dore,¹⁴
J. Dumarchez,¹⁵ R. Edgecock,¹⁶ M. Ellis,^{16, f} F. Ferri,⁸ U. Gastaldi,¹⁷ S. Giani,² G. Giannini,¹
D. Gibin^(**),⁶ S. Gilardoni,² P. Gorbunov,^{2, b} C. Gößling,¹⁸ J.J. Gómez–Cadenas,¹¹ A. Grant,²
J.S. Graulich,^{19, g} G. Grégoire,¹⁹ V. Grichine,³ A. Grossheim,^{2, h} A. Guglielmi^(*),⁶ L. Howlett,⁹
A. Ivanchenko,^{2, i} V. Ivanchenko,^{2, j} A. Kayis-Topaksu,^{2, k} M. Kirsanov,²⁰ D. Kolev,⁷ A. Krasnoperov,¹⁰
J. Martín–Albo,¹¹ C. Meurer,²¹ M. Mezzetto^(*),⁶ G. B. Mills,^{· l} M.C. Morone,^{5, m} P. Novella,¹¹
D. Orestano^(**),²² V. Palladino,²³ J. Panman,² I. Papadopoulos,² F. Pastore^(**),²² S. Piperov,²⁴
N. Polukhina,³ B. Popov,^{10, n} G. Prior,^{5, d} E. Radicioni,¹² D. Schmitz,^{· o} R. Schroeter,⁵ G. Skoro,⁹
M. Sorel,¹¹ E. Tcherniaev,² P. Temnikov,²⁴ V. Tereschenko,¹⁰ A. Tonazzo^(**),²² L. Tortora^(*),²²
R. Tsenov,⁷ I. Tsukerman,^{2, b} G. Vidal–Sitjes,^{13, a} C. Wiebusch,^{2, p} and P. Zucchelli^{2, q}

¹*Università degli Studi e Sezione INFN, Trieste, Italy*

²*CERN, Geneva, Switzerland*

³*P. N. Lebedev Institute of Physics (FIAN),
Russian Academy of Sciences, Moscow, Russia*

⁴*Nuclear and Astrophysics Laboratory, University of Oxford, UK*

⁵*Section de Physique, Université de Genève, Switzerland*

⁶*Sezione INFN^(*) and Università degli Studi^(**), Padova, Italy*

⁷*Faculty of Physics, St. Kliment Ohridski University,
Sofia, Bulgaria*

⁸*Sezione INFN Milano Bicocca, Milano, Italy*

⁹*Dept. of Physics, University of Sheffield, UK*

¹⁰*Joint Institute for Nuclear Research, JINR Dubna, Russia*

¹¹*Instituto de Física Corpuscular, IFIC, CSIC and Universidad de Valencia, Spain*

¹²*Sezione INFN, Bari, Italy*

¹³*Università degli Studi e Sezione INFN, Ferrara, Italy*

¹⁴*Università “La Sapienza” e Sezione INFN Roma I, Roma, Italy*

¹⁵*LPNHE, Universités de Paris VI et VII, Paris, France*

¹⁶*Rutherford Appleton Laboratory, Chilton, Didcot, UK*

¹⁷*Laboratori Nazionali di Legnaro dell’ INFN, Legnaro, Italy*

¹⁸*Institut für Physik, Universität Dortmund, Germany*

¹⁹*Institut de Physique Nucléaire, UCL, Louvain-la-Neuve, Belgium*

²⁰*Institute for Nuclear Research, Moscow, Russia*

²¹*Institut für Physik, Forschungszentrum Karlsruhe, Germany*

²²*Sezione INFN^(*) and Università^(**) Roma Tre, Roma, Italy*

²³*Università “Federico II” e Sezione INFN, Napoli, Italy*

²⁴*Institute for Nuclear Research and Nuclear Energy, Academy of Sciences,
Sofia, Bulgaria*

I. INTRODUCTION

In many particle and astroparticle physics experiments the knowledge of hadron production is required as an external input to make optimal use of the recorded data and to help design the experimental facilities. The HARP experiment [1] is motivated by this need for precise hadron production measurements. It has taken data with beams of pions and protons with momenta from 1.5 GeV/c to 15 GeV/c hitting nuclear targets made of a large range of materials. To provide a large angular and momentum coverage of the produced charged particles the experiment comprises two spectrometers, a forward spectrometer built around a dipole magnet covering the angular range up to 250 mrad and a large-angle spectrometer constructed in a solenoidal magnet with an angular acceptance of $0.35 \text{ rad} \leq \theta < 2.15 \text{ rad}$, based on a time-projection-chamber (TPC).

The main HARP objectives are to measure pion yields for a quantitative design of the proton driver of future superbeams (high-intensity conventional beams) and a neutrino factory [2], to provide measurements to improve calculations of the atmospheric neutrino flux [3–6] and to measure particle yields as input for the flux calculation of accelerator neutrino experiments [7], such as K2K [8, 9], MiniBooNE [10] and SciBooNE [11]. The momentum range of the incoming particles presented here corresponds to a momentum region of great interest for neutrino beams and are in a region far from coverage by earlier dedicated hadroproduction experiments [12, 13]. In addition to these specific aims, the data provided by HARP are valuable for validating hadron production models used in sim-

ulation programs. These simulations are playing an important role in the interpretation and design of modern particle-physics experiments. In particular, the simulation of calorimeter response and secondary interactions in tracking systems needs to be supported by experimental hadron production data. Results on forward production of charged pions by incident protons are the subject of previous HARP publications [14–18]. The analysis of results on charged pion production with charged pion beams on the full range of targets can be found in Ref. [19]¹.

In this paper, measurements of the double-differential cross-section, $d^2\sigma^p/dpd\Omega$, for forward production of protons by incident charged pions or protons of 3 GeV/c, 5 GeV/c, 8 GeV/c, 8.9 GeV/c (Be only), 12 GeV/c and 12.9 GeV/c (Al only) momentum impinging on a thin solid beryllium, carbon, aluminium, copper, tin, tantalum and lead targets of 5% nuclear interaction length (λ_I) thickness are presented.

To our knowledge no high statistics proton production data at low momenta ($\leq 15 \text{ GeV}/c$) in the forward direction ($\leq 250 \text{ mrad}$) with incident protons or charged pions on nuclear targets have been published.

Data were taken in the T9 beam of the CERN PS. The collected statistics, for the different nuclear targets, are reported in Table I.

A. Experimental apparatus

The HARP experiment makes use of a large-acceptance spectrometer consisting of a forward and a large-angle detection system. The HARP detector is shown in Fig. 1 and is fully described in Ref. [22]. The forward spectrometer – based on five modules of large area drift chambers (NDC1-5) [23] and a dipole magnet complemented by a set of detectors for particle identification (PID): a time-of-flight wall (TOFW) [24], a large Cherenkov detector (CHE) and an electromagnetic calorimeter (ECAL) – covers polar angles up to 250 mrad, which is well matched to the angular range of interest for the measurement of hadron production to calculate the properties of conventional neutrino beams. The discrimination power of time-of-flight below 3 GeV/c and the Cherenkov detector above 3 GeV/c are combined to provide power-

^aNow at Imperial College, University of London, UK.

^bITEP, Moscow, Russian Federation.

^cCorresponding author (M. Bonesini).

E-mail: maurizio.bonesini@mib.infn.it

^dNow at CERN

^eColumbia University, New York, USA (MiniBooNE Coll).

Now at University of California, Riverside, USA.

^fNow at FNAL, Batavia, Illinois, USA.

^gNow at Section de Physique, Université de Genève, Switzerland.

^hNow at TRIUMF, Vancouver, Canada.

ⁱNow at CNRS, CENBG Bordeaux, France.

^jOn leave from Ecoanalitica, Moscow State University, Moscow, Russia

^kNow at Çukurova University, Adana, Turkey.

^lLos Alamos National Laboratory, Los Alamos, USA (MiniBooNE Coll.)

^mNow at University of Rome Tor Vergata, Italy.

ⁿAlso supported by LPNHE, Paris, France.

^oColumbia University, New York, USA (MiniBooNE Coll.)

^pNow at III Phys. Inst. B, RWTH Aachen, Germany.

^qNow at SpinX Technologies, Geneva, Switzerland;
on leave from INFN, Sezione di Ferrara, Italy.

¹ results on the large angle charged pion production are instead presented in Refs. [20] and [21]

TABLE I: Total number of events and tracks used in the various nuclear 5% λ_I target data sets and the number of incident protons and charged pions on target as calculated from the pre-scaled incident beam triggers. First entries (total DAQ events) are for the positive and negative beam; then numbers are given for incident protons, π^+ , π^- in units of 10^3 events.

Data set (GeV/c)		3		5		8		8.9		12		12.9	
beam polarity		+	-	+	-	+	-	+	-	+	-	+	
Total DAQ events	(Be)	1113	2233	1296	1798	1935	1585	5868		1207	1227		
	(C)	1345	1831	2628	1279	1846	1399			1062	646		
	(Al)	1159	1523	1789	920	1707	1059			619	741	4713	
	(Cu)	624	3325	2079	1805	2089	1615			745	591		
	(Sn)	1637	1972	2828	1625	2404	1408			1803	937		
	(Ta)	1783	994	2084	1435	1965	1505			866	961		
	(Pb)	1911	1282	2111	2074	2266	1496			487	1706		

Data set (GeV/c)		3			5			8			8.9		12			12.9	
particle type		p	π^+	π^-	p	π^+	π^-	p	π^+	π^-	p	π^+	p	π^+	π^-	p	π^+
Acc. beam part.	(Be)	99	246	731	289	384	914	761	341	826	2103	1278	580	76	693		
with forw. int.	(C)	101	257	299	542	754	530	709	358	772			470	41	352		
	(Al)	86	213	486	376	523	308	637	335	611			306	27	435	2116 332	
	(Cu)	73	168	1185	408	611	850	741	397	966			363	33	347		
	(Sn)	217	467	778	528	819	732	818	481	804			856	79	584		
	(Ta)	281	561	426	398	600	671	668	388	893			403	37	536		
	(Pb)	310	611	473	387	594	997	758	444	896			221	20	839		

Final state p		3			5			8			8.9		12			12.9	
selected with PID		p	π^+	π^-	p	π^+	π^-	p	π^+	π^-	p	π^+	p	π^+	π^-	p	π^+
	(Be)	7.2	1.7	1.5	18.0	3.8	3.1	37.0	4.3	4.8	86.4	15.6	19.3	1.0	5.7		
	(C)	6.2	1.6	0.6	29.1	6.7	1.7	32.2	4.4	4.1			14.8	0.5	2.5		
	(Al)	4.2	1.3	0.8	19.0	4.8	1.0	26.8	3.9	2.9			10.6	0.4	2.8	73.3 5.0	
	(Cu)	2.5	0.8	1.6	18.1	5.6	2.9	31.5	5.2	6.0			12.9	0.6	3.1		
	(Sn)	4.9	1.5	0.9	20.8	6.9	2.5	33.6	6.4	3.9			30.2	1.3	5.2		
	(Ta)	4.8	1.4	0.4	12.9	4.6	2.1	25.6	5.0	4.2			14.2	0.6	4.8		
	(Pb)	4.4	1.4	0.3	12.0	4.0	2.8	26.6	5.2	4.4			7.5	0.3	7.4		

ful separation of forward pions and protons [25]. The calorimeter is used only for separating pions and electrons when characterizing the response of the other detectors. The muon contamination of the beam is measured with a 1.4 m wide muon identifier (BMI). At the downstream end of the spectrometer, after a 0.4 m long iron absorber, it is made of an iron-scintillator sandwich with five planes of six scintillator each, read out at both sides, giving a total thickness of $6.4 \lambda_I$.

The large-angle spectrometer consists of a Time Projection Chamber (TPC) and Resistive Plate Chambers (RPCs), located inside a solenoidal magnet. It has a large acceptance in the momentum and angular range for the pions relevant to the production of the muons in a neutrino factory. This system is not used in the present analysis.

The HARP experiment, located in the T9 beam of the CERN PS, took data in 2001 and 2002. The momentum definition of the T9 beam is known with a precision of the order of 1% [26].

The target is placed inside the inner field cage (IFC) of the TPC, in an assembly that can be moved in and out of the solenoid magnet. The solid targets used for the measurements reported here have a cylindrical shape with a nominal diameter of about 30 mm. Their thickness is equivalent to about 5% of λ_I .

A set of four multi-wire proportional chambers (MWPCs) measures the position and direction of the incoming beam particles with an accuracy of ≈ 1 mm in position and ≈ 0.2 mrad in angle per projection. A beam time-of-flight system (BTOF) measures the time difference of particles over a 21.4 m path-length. It is made of two identical scintillation hodoscopes, TOFA and TOFB (originally built for the NA52 experiment [27]), which, together with a small target-defining trigger counter (TDS, also used for the trigger), provide particle identification at low energies. This provides separation of pions, kaons and protons up to 5 GeV/c and determines the initial time at the interaction vertex (t_0). The timing resolution of

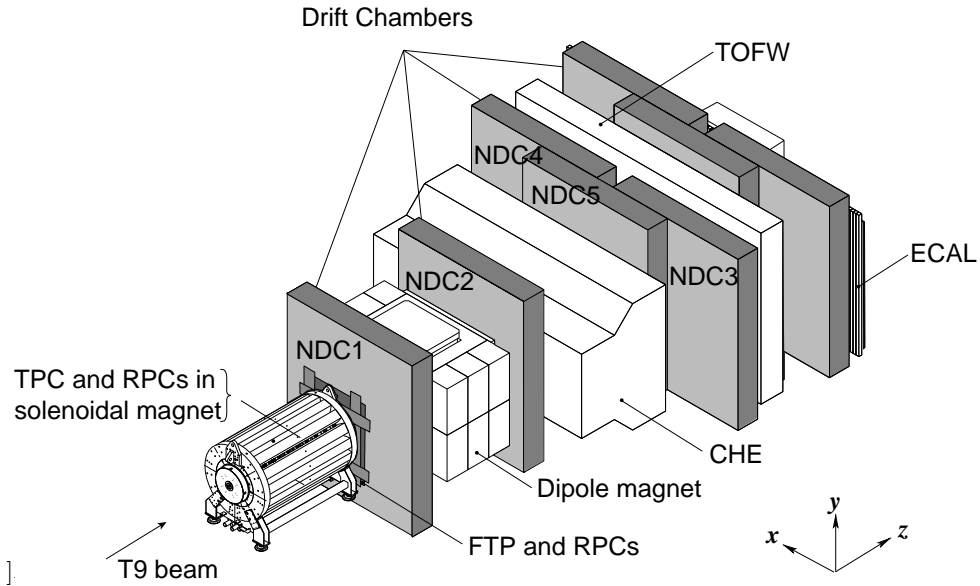


FIG. 1: Schematic layout of the HARP detector. The convention for the coordinate system is shown in the lower-right corner. The three most downstream (unlabelled) drift chamber modules are only partly equipped with electronics and are not used for tracking. The detector covers a total length of 13.5 m along the beam axis and has a maximum width of 6.5 m perpendicular to the beam. The beam muon identifier is visible as the most downstream detector (white box).

the combined BTOF system is about 70 ps. A system of two N_2 -filled Cherenkov detectors (BCA and BCB) is used to tag electrons at low energies and pions at higher energies. The electron and pion tagging efficiency is found to be close to 100%. At the beam energy used for this analysis the Cherenkov counters select all particles lighter than protons, while the BTOF is used to reject ions. A set of trigger detectors completes the beam instrumentation.

The beam of positive particles used for this measurement contains mainly positrons, muons, pions and protons, with small components of kaons, deuterons and heavier ions. Its composition depends on the selected beam momentum. The proton fraction in the incoming positive-particle beam varies from $\sim 35\%$ at 3 GeV/ c to $\sim 92\%$ at 12 GeV/ c . The negatively-charged particle beam is mainly composed of pions with small background components of muons and electrons.

At the first stage of the analysis a favoured beam particle type is selected using the beam time-of-flight system and the two Cherenkov counters. A value of the pulse height consistent with the absence of a signal in both beam Cherenkov detectors distinguishes protons (and kaons) from electrons and pions. We also ask for time measurements to be present which are needed for calculating the arrival time of the beam proton at the target. The beam TOF system is used to reject ions, such as deuterons, and to separate protons

from pions at low momenta. At 3 GeV/ c , the TOF measurement allows the selection of pions from protons to be made at more than 5σ . In most beam settings the nitrogen pressure in the beam Cherenkov counters was too low for kaons to be above the threshold. Kaons are thus contained in the proton sample. However, the fraction of kaons has been measured in the 12.9 GeV/ c beam configuration and is found to contribute less than 0.5%, and hence it is negligible both in the pion and proton beam sample. Electrons radiate in the Cherenkov counters and would be counted as pions. In the 3 GeV/ c beam, electrons are identified by both Cherenkov counters, since the pressure was such that pions remained below threshold. In the 5 GeV/ c beam electrons could be tagged by one Cherenkov counter only, while the other Cherenkov counter was used to tag pions. The e/π fraction was measured to be 1% in the 3 GeV/ c beam and $< 10^{-3}$ in the 5 GeV/ c beam. By extrapolation from the lower-energy beam settings this electron contamination can be estimated to be negligible ($< 10^{-3}$) for the beams where it cannot be measured directly. More details on the beam particle selection can be found in [14] and Refs. [22].

In addition to the momentum-selected beam of protons and pions originating from the T9 production target one expects also the presence of muons from pion decay both downstream and upstream of the beam momentum selection. Therefore, precise absolute knowledge of the muon rate incident on the HARP targets is required when measure-

ments of particle production with incident pions are performed. The particle identification detectors in the beam do not distinguish muons from pions. A separate measurement of the muon component has been performed using data-sets without target (“empty-target data-sets”). Since the empty-target data were taken with the same beam parameter settings as the data taken with targets, the beam composition can be measured in the empty-target runs using the forward spectrometer and then used as an overall correction for the counting of pions in the runs with targets. Muons are recognized by their longer range in the beam muon identifier (BMI). The punch-through background in the BMI is measured counting the protons (identified with the beam detectors) thus mis-identified as muons by the BMI. A comparison of the punch-through rate between simulated incoming pions and protons was used to determine a correction for the difference between pions and protons and to determine the systematic error. This difference is the dominant systematic error in the beam composition measurement. The aim was to determine the composition of the beam as it strikes the target, thus muons produced in pion decays after the HARP target should be considered as a background to the measurement of muons in the beam. The rate of these latter background muons, which depends mainly on the total inelastic cross-section and pion decay, was calculated by a Monte Carlo simulation using GEANT4 [28]. The muon fraction in the beam (at the target) is obtained taking into account the efficiency of the BMI selection criteria as well as the punch-through and decay backgrounds. The analyses for the various beam settings give results for $R = \mu/(\mu + \pi)$ of $(4.2 \pm 1)\%$ and $(5.2 \pm 1)\%$ for the low-momentum beams (3 GeV/c and 5 GeV/c) and between $(4.1 \pm 1)\%$ and $(2.8 \pm 1)\%$ for the highest momenta (from 8 GeV/c to 12.9 GeV/c). The uncertainty in these fractions is dominated by the systematic uncertainty in the punch-through background. The fact that the background does not scale with the decay probability for pions is due to the limited acceptance of the beam-line to transport the decay muons. The muon contamination is taken into account in the normalization of the pion beam and adds a systematic error of 1% to the overall normalization. Only events with a single reconstructed beam track in the four MWPCs, good timing measurements in BTOF and no signal in the beam halo counters are accepted.

A downstream trigger in the forward scintillator trigger plane (FTP) was required to record an event, accepting only tracks with a trajectory outside the central hole (60 mm) which allows beam particles to pass.

The length of the accelerator spill is 400 ms with a

typical intensity of 15 000 beam particles per spill. The average number of events recorded by the data acquisition ranges from 300 to 350 per spill.

The absolute normalization of the cross-section was performed using “incident-proton” triggers. These are triggers where the same selection on the beam particle was applied but no selection on the interaction was performed. The rate of this trigger was down-scaled by a factor 64. These unbiased events are used to determine N_{pot} in the cross-section formula (1), see later.

II. DATA ANALYSIS AND CROSS-SECTION CALCULATION.

This analysis is similar to the one reported in reference [19]. For the current analysis we have used identical reconstruction and PID algorithms. Secondary track selection criteria, described in [16], are optimized to ensure the quality of momentum reconstruction and a clean time-of-flight measurement while maintaining a high reconstruction efficiency.

The background induced by interactions of beam particles in the materials outside the target is measured by taking data without a target in the target holder (“empty target data”). These data are subject to the same event and track selection criteria as the standard data sets and are subtracted bin-by-bin.

The collected event statistics on the different solid targets is summarised in Table I.

The double-differential cross-section for the production of a particle of type α is calculated as follows:

$$\frac{d^2\sigma^\alpha}{dpd\Omega}(p_i, \theta_j) = \frac{A}{N_A \rho t} \cdot \frac{1}{N_{\text{pot}}} \cdot \frac{1}{\Delta p_i \Delta \Omega_j} \cdot \sum_{p'_i, \theta'_j, \alpha'} \mathcal{M}_{p_i \theta_j \alpha p'_i \theta'_j \alpha'}^{\text{cor}} \cdot N^{\alpha'}(p'_i, \theta'_j), \quad (1)$$

where

- $\frac{d^2\sigma^\alpha}{dpd\Omega}(p_i, \theta_j)$ is the cross-section in mb/(GeV/c sr) for the particle type α (a proton in our case) for each true momentum and angle bin (p_i, θ_j) covered in this analysis;
- $N^{\alpha'}(p'_i, \theta'_j)$ is the number of particles of type α' in bins of reconstructed momentum p'_i and angle θ'_j in the raw data, after subtraction of empty target data (due to beam protons

interacting in material other than the nuclear target). These particles must satisfy the event, track and PID selection criteria.

- $M_{p\theta\alpha p'\theta'\alpha'}^{\text{cor}}$ is the correction matrix which accounts for finite efficiency and resolution of the detector. It unfolds the true variables p_i, θ_j, α from the reconstructed variables p'_i, θ'_j, α' and corrects the observed particle number to take into account effects such as reconstruction efficiency, acceptance, absorption, pion decay, tertiary production, PID efficiency and PID misidentification rate.
- $\frac{A}{N_A \rho t}$, $\frac{1}{N_{\text{pot}}}$ and $\frac{1}{\Delta p_i \Delta \Omega_j}$ are normalization factors, namely:

$\frac{N_A \rho t}{A}$ is the number of target nuclei per unit area ²;

N_{pot} is the number of protons on target (particles on target);

Δp_i and $\Delta \Omega_j$ are the bin sizes in momentum and solid angle, respectively ³.

We do not make a correction for the attenuation of the beam in the target, so that strictly speaking the cross-sections are valid for $\lambda_I = 5\%$ targets.

The calculation of the correction matrix $M_{p_i\theta_j\alpha p'_i\theta'_j\alpha'}^{\text{cor}}$ is a rather difficult task. Various techniques are described in the literature to obtain this matrix. The method applied here and called UFO in [14] is the unfolding method introduced by D'Agostini [29] ⁴.

The Monte Carlo simulation of the HARP setup is based on GEANT4 [28]. The detector materials are accurately described in this simulation as well

as the relevant features of the detector response and the digitization process. All relevant physics processes are considered, including multiple scattering, energy loss, absorption and re-interactions. The track reconstruction used in this analysis and the simulation are identical to the ones used for the π^+ production in p-Be collisions [15]. A detailed description of the corrections and their magnitude can be found there.

The reconstruction efficiency (inside the geometrical acceptance) is larger than 95% above 1.5 GeV/c and drops to 80% at 0.5 GeV/c. The requirement of a match with a TOFW hit has an efficiency between 90% and 95% independent of momentum. The electron veto rejects about 1% of the pions and protons below 3 GeV/c with a remaining background of less than 0.5%. Below Cherenkov threshold the TOFW separates pions and protons with negligible background and an efficiency of $\approx 94\%$ for protons at low momentum increasing to $\approx 98\%$ at threshold. Above Cherenkov threshold the efficiency for protons is greater than 98% with less than 1% of pions mis-identified as protons.

The absorption and decay of particles is simulated by the Monte Carlo. The absorption correction is on average 20%, approximately independent of momentum. Uncertainties in the absorption of secondaries in the dipole spectrometer material are taken into account by a variation of 10% of this effect in the simulation. The uncertainty in the production of background due to tertiary particles is larger. The average correction is $\approx 10\%$ and up to 20% at 1 GeV/c. The correction includes reinteractions in the detector material as well as a small component coming from reinteractions in the target. The validity of the generators used in the simulation was checked by an analysis of HARP data with incoming protons and charged pions on aluminium and carbon targets at lower momenta (3 GeV/c and 5 GeV/c). A 30% variation of the secondary production was applied. The average empty-target subtraction amounts to $\approx 20\%$.

Owing to the redundancy of the tracking system downstream of the target the detection efficiency is very robust under the usual variations of the detector performance during the long data taking periods. Since the momentum is reconstructed without making use of the upstream drift chamber module (which is more sensitive in its performance to the beam intensity) the reconstruction efficiency is uniquely determined by the downstream system. No variation of the overall efficiency has been observed. The performance of the TOFW and CHE system have been monitored to be constant for the data taking periods used in this analysis. The calibration of the detectors was performed on a day-by-day basis.

² A - atomic mass, N_A - Avogadro number, ρ - target density and t - target thickness

³ $\Delta p_i = p_i^{\text{max}} - p_i^{\text{min}}$, $\Delta \Omega_j = 2\pi(\cos(\theta_j^{\text{min}}) - \cos(\theta_j^{\text{max}}))$

⁴ The unfolding method tries to put in correspondence the vector of measured observables (such as particle momentum, polar angle and particle type) x_{meas} with the vector of true values x_{true} using a migration matrix: $x_{\text{meas}} = M_{\text{migr}} \times x_{\text{true}}$. The goal of the method is to compute a transformation (correction matrix) to obtain the expected values for x_{true} from the measured ones. The most simple and obvious solution, based on simple matrix inversion M_{migr}^{-1} , is usually unstable and is dominated by large variances and strong negative correlations between neighbouring bins. In the method of D'Agostini, the correction matrix M^{UFO} tries to connect the measurement space (effects) with the space of the true values (causes) using an iterative Bayesian approach, based on Monte Carlo simulations to estimate the probability for a given effect to be produced by a certain cause.

A. Error estimation

The total statistical error of the corrected data is composed of the statistical error of the raw data and of the statistical error of the unfolding procedure, as the unfolding matrix is obtained from the data themselves, thus contributing also to the statistical error. The statistical error provided by the unfolding program is equivalent to the propagated statistical error of the raw data. In order to calculate the statistical error of the unfolding procedure a separate analysis is applied, as described in [16],[30]. Its conclusion is that the statistical error provided by the unfolding procedure has to be multiplied globally by a factor of 2, which is done for the analyses described here. This factor is somewhat dependent on the shape of the distributions.

Different types of sources induce systematic errors for the analysis described here: track yield corrections ($\sim 5\%$), particle identification ($\sim 0.1\%$), momentum and angular reconstruction ($\sim 1\%$)⁵. The strategy to calculate these systematic errors and the different methods used for their evaluation are fully described in [16]. As a result of these systematic error studies, each error source can be represented by a covariance matrix. The sum of these matrices describes the total systematic error, as explained in [16].

The experimental uncertainties are shown for a typical target (Be) in Figure 2 at 5 GeV/c and 12 GeV/c incident beam momenta for incident protons and negative pions. They are very similar for π^+ and at the other beam energies. Going from lighter (Be, C) to heavier targets (Ta, Pb) the corrections for π^0 (conversion) and absorption/tertiaries increase.

On average the total integrated systematic error is around 5 – 6%, with a differential bin-to-bin systematic error of the order of 10 – 11%, to be compared with a statistical integrated (bin-to-bin differential) error of $\sim 2 - 3\%$ ($\sim 10 - 13\%$). Systematic and statistical errors are roughly of the same order.

⁵ The quoted error in parenthesis refers to fractional error of the integrated cross-section ($\delta_{\text{int}}^{\pi}(\%)$) in the kinematic range covered by the HARP experiment

III. EXPERIMENTAL RESULTS

The measured double-differential cross-sections for the production of forward protons in the laboratory system as a function of the momentum and the polar angle for each incident beam momentum are shown in Figures 3 and 4 for two typical solid targets: beryllium and lead, as an example of a light and a heavy target. The error bars shown are the square-roots of the diagonal elements in the covariance matrix, where statistical and systematic uncertainties are combined in quadrature. The correlation of the statistical errors (introduced by the unfolding procedure) are typically smaller than 20% for adjacent momentum bins and even smaller for adjacent angular bins. The correlations of the systematic errors are larger, typically 80% for adjacent bins. The overall scale error ($< 2\%$) is not shown. The results of the analysis for all solid targets are fully tabulated in Appendix A⁶.

The dependence of the averaged proton yields on the incident beam momentum is shown in Fig. 5. The proton yields, averaged over two angular regions ($0.05 \text{ rad} \leq \theta < 0.15 \text{ rad}$ and $0.15 \text{ rad} \leq \theta < 0.25 \text{ rad}$) and four momentum regions ($0.5 \text{ GeV}/c \leq p < 1.5 \text{ GeV}/c$, $1.5 \text{ GeV}/c \leq p < 2.5 \text{ GeV}/c$, $2.5 \text{ GeV}/c \leq p < 3.5 \text{ GeV}/c$ and $3.5 \text{ GeV}/c \leq p < 4.5 \text{ GeV}/c$), are shown.

The dependence of the averaged proton yields on the atomic number A is shown in Fig. 6. The yields are shown, averaged over two angular regions ($0.05 \text{ rad} \leq \theta < 0.15 \text{ rad}$ and $0.15 \text{ rad} \leq \theta < 0.25 \text{ rad}$) and four momentum regions ($0.5 \text{ GeV}/c \leq p < 1.5 \text{ GeV}/c$, $1.5 \text{ GeV}/c \leq p < 2.5 \text{ GeV}/c$, $2.5 \text{ GeV}/c \leq p < 3.5 \text{ GeV}/c$ and $3.5 \text{ GeV}/c \leq p < 4.5 \text{ GeV}/c$).

The particle production ratios π^-/π^+ and π^+/p , in the integrated angular range $0.05 \text{ rad} \leq \theta < 0.25 \text{ rad}$, are reported instead in Figures 7 and 8 for two typical targets: beryllium and tantalum and the different incident beam particles. They clearly reflect the charge polarity of the incident beam particle, especially at high secondary momenta.

⁶ the scale error has not been included to make it possible to calculate e.g. integrated particle ratios taking it into account only when applicable, i.e. when different beams are compared.

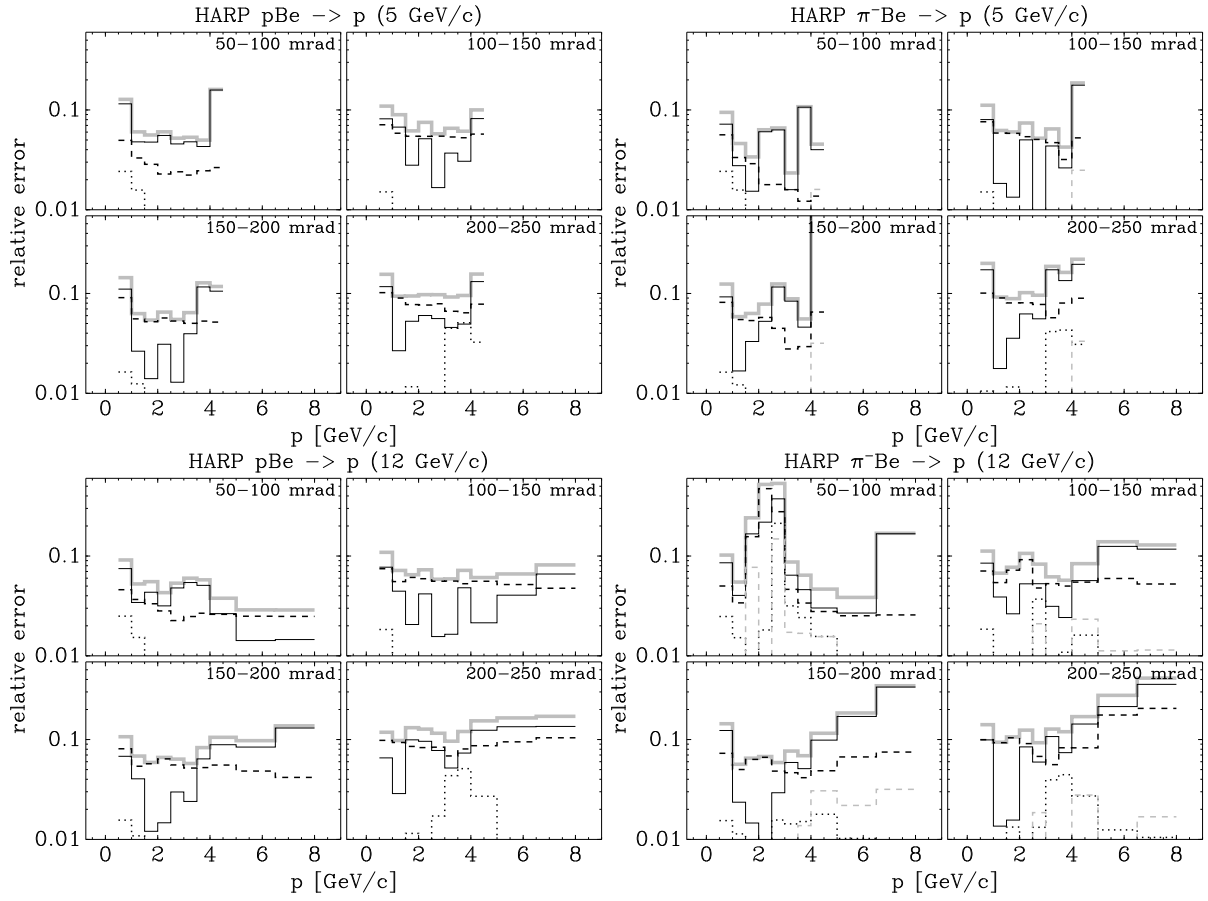


FIG. 2: Total systematic error (grey solid line) and main components for a typical (Be) target with incident p and π^- beams at 5 and 12 GeV/c black short-dashed line for absorption+tertiaries interactions, black dotted line for track efficiency and target pointing efficiency, black dot-dashed line for π^0 subtraction, black solid line for momentum scale+resolution and angle scale, grey short-dashed line for PID.

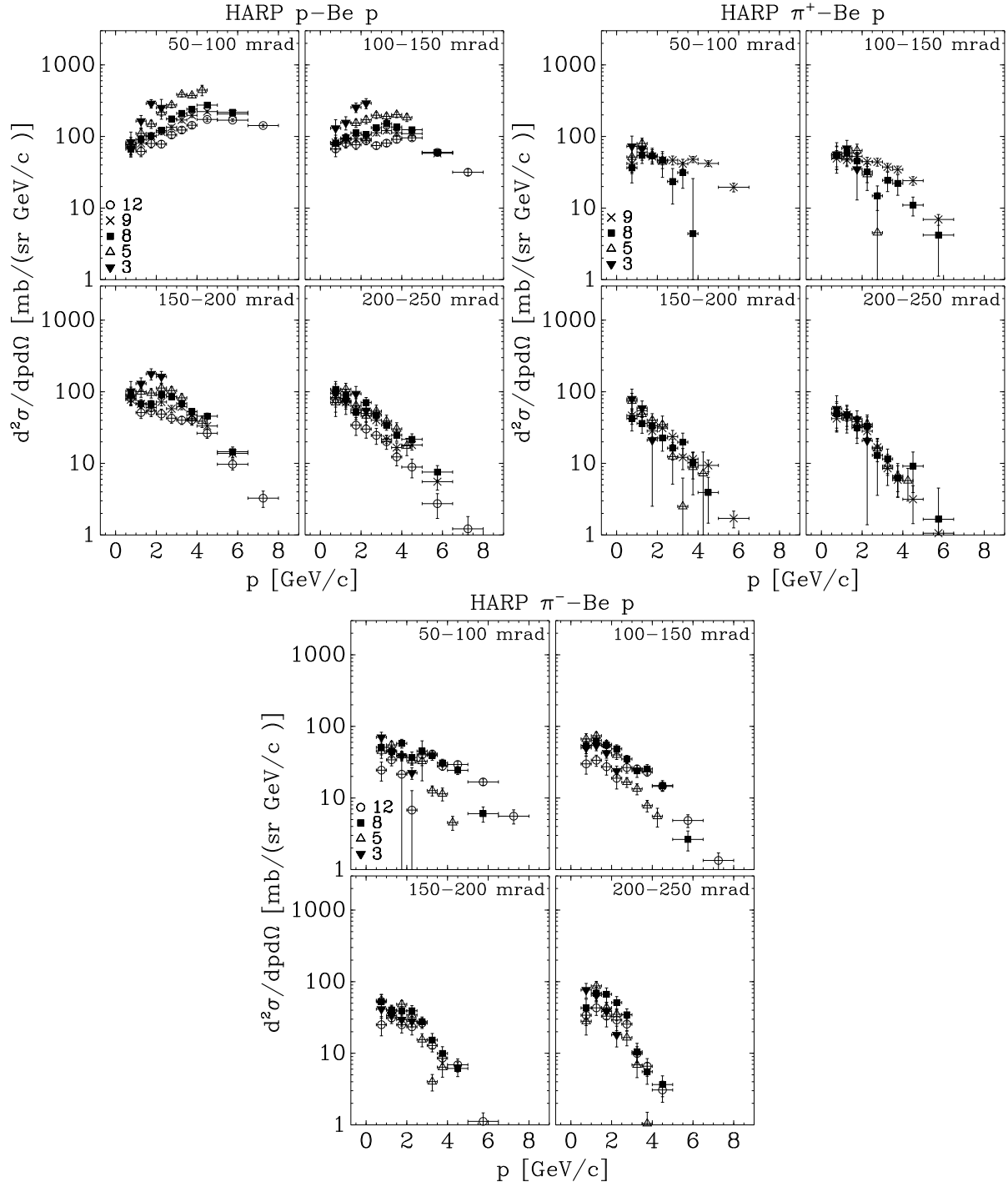


FIG. 3: Differential cross sections for proton forward production with incident p , π^{\pm} on a thin Be target. In the top right corner of each plot the covered angular range is shown in mrad.

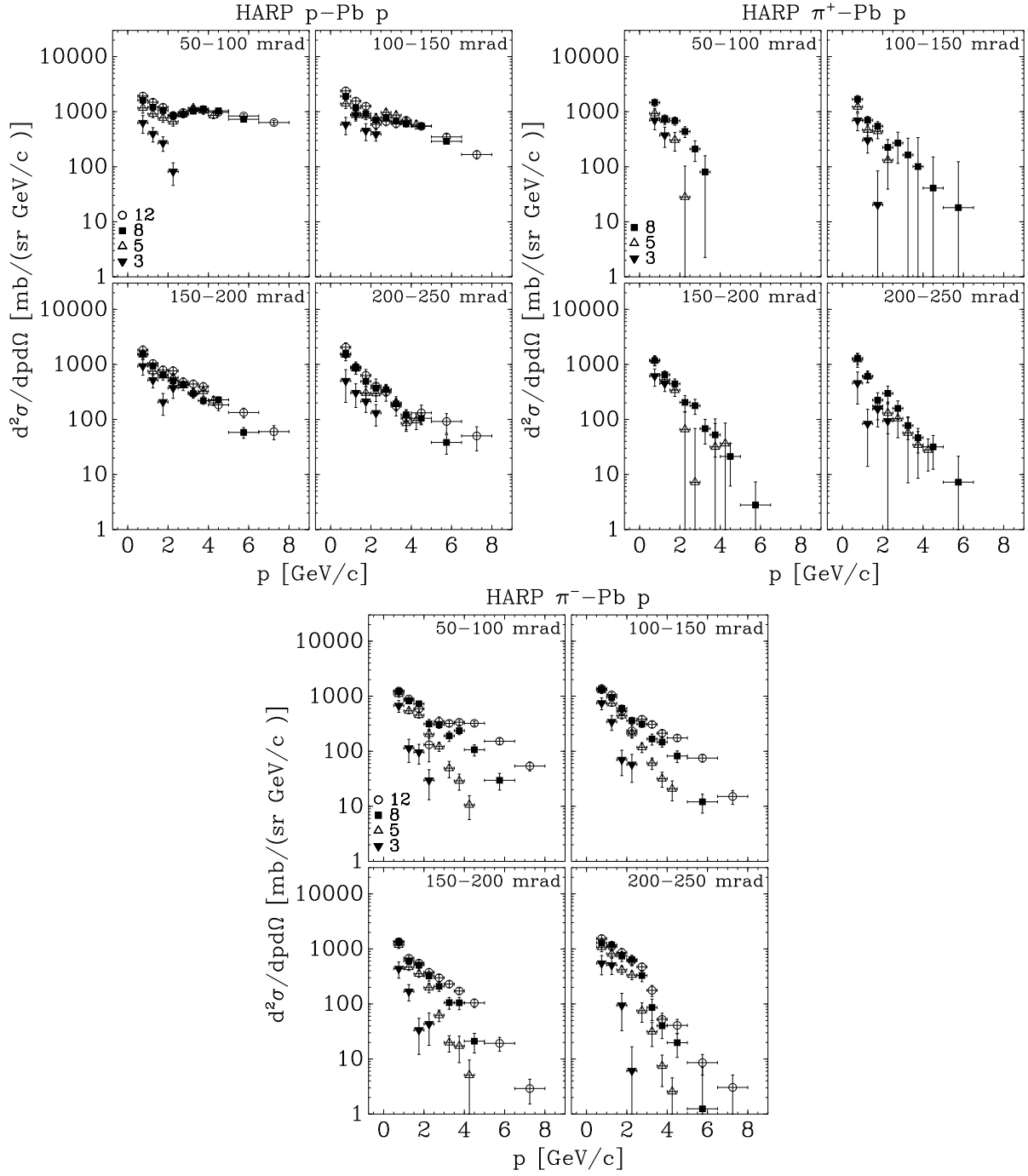


FIG. 4: Differential cross sections for proton forward production with incident p , π^\pm on a thin Pb target. In the top right corner of each plot the covered angular range is shown in mrad.

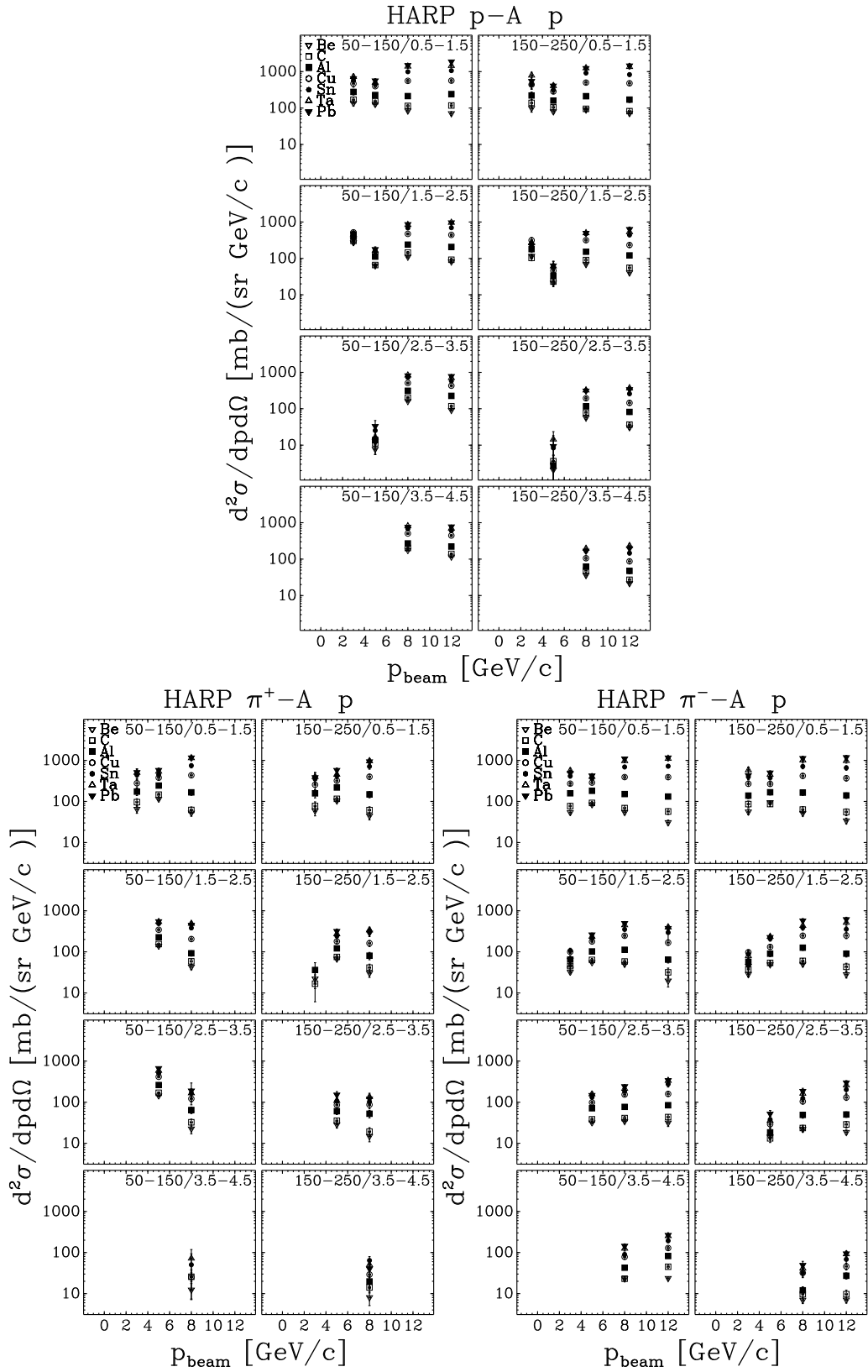


FIG. 5: The dependence on the beam momentum of the forward proton production yields in p-A and π^\pm -A (A = Be,C,Al,Cu,Sn,Ta, Pb) interactions averaged over two forward angular regions ($0.05 \text{ rad} \leq \theta < 0.15 \text{ rad}$ and $0.15 \text{ rad} \leq \theta < 0.25 \text{ rad}$) and four momentum regions ($0.5 \text{ GeV}/c \leq p < 1.5 \text{ GeV}/c$, $1.5 \text{ GeV}/c \leq p < 2.5 \text{ GeV}/c$, $2.5 \text{ GeV}/c \leq p < 3.5 \text{ GeV}/c$ and $3.5 \text{ GeV}/c \leq p < 4.5 \text{ GeV}/c$), for the four different incoming beam energies.

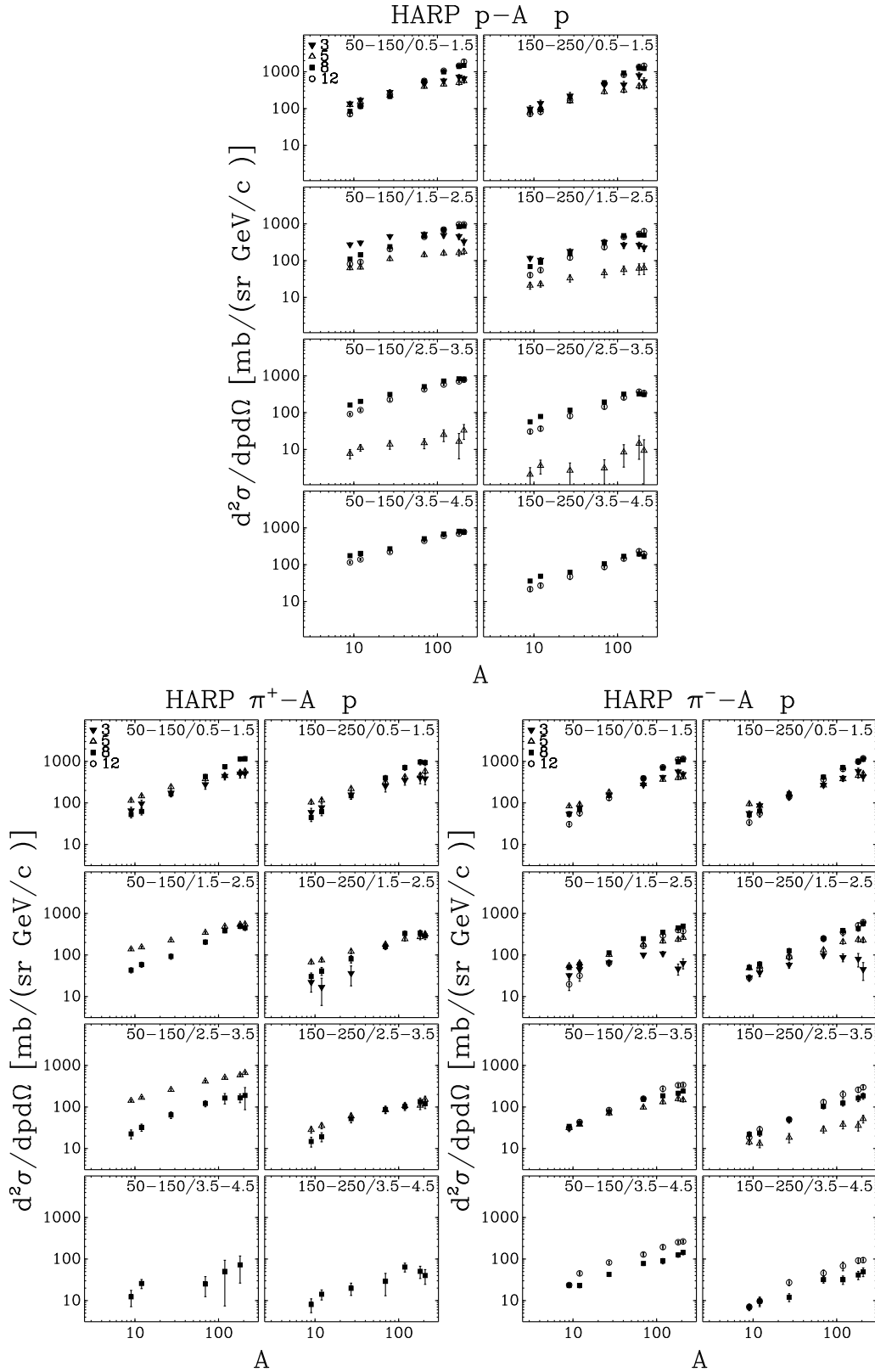


FIG. 6: The dependence on the atomic number A of the forward proton production yields in $p-A$ and $\pi^\pm-A$ ($A=\text{Be,Al,C,Cu,Sn,Ta,Pb}$) interactions averaged over two forward angular regions ($0.05 \text{ rad} \leq \theta < 0.15 \text{ rad}$ and $0.15 \text{ rad} \leq \theta < 0.25 \text{ rad}$) and four momentum regions ($0.5 \text{ GeV}/c \leq p < 1.5 \text{ GeV}/c$, $1.5 \text{ GeV}/c \leq p < 2.5 \text{ GeV}/c$, $2.5 \text{ GeV}/c \leq p < 3.5 \text{ GeV}/c$ and $3.5 \text{ GeV}/c \leq p < 4.5 \text{ GeV}/c$), for the four different incoming beam energies.

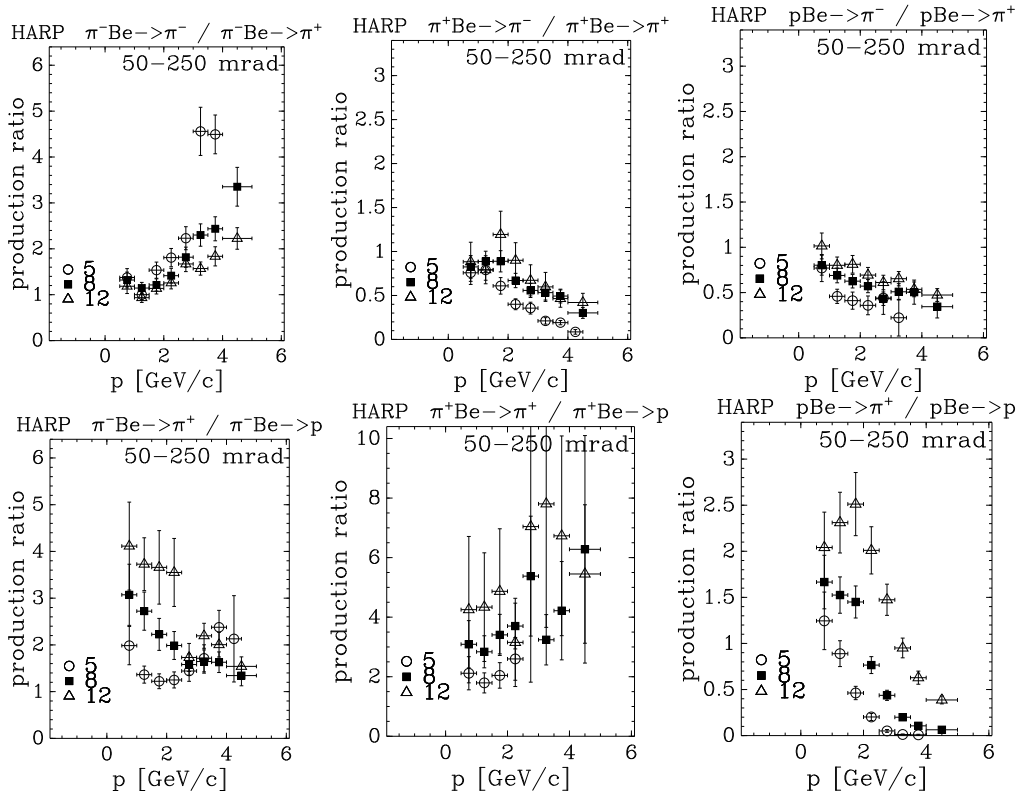


FIG. 7: Particle production ratios on a Be target at 5, 8, 12 GeV/c. Top panels: π^-/π^+ ratio with incident π^- , π^+ and p; bottom panels: π^+/p ratio with incident π^- , π^+ and p.

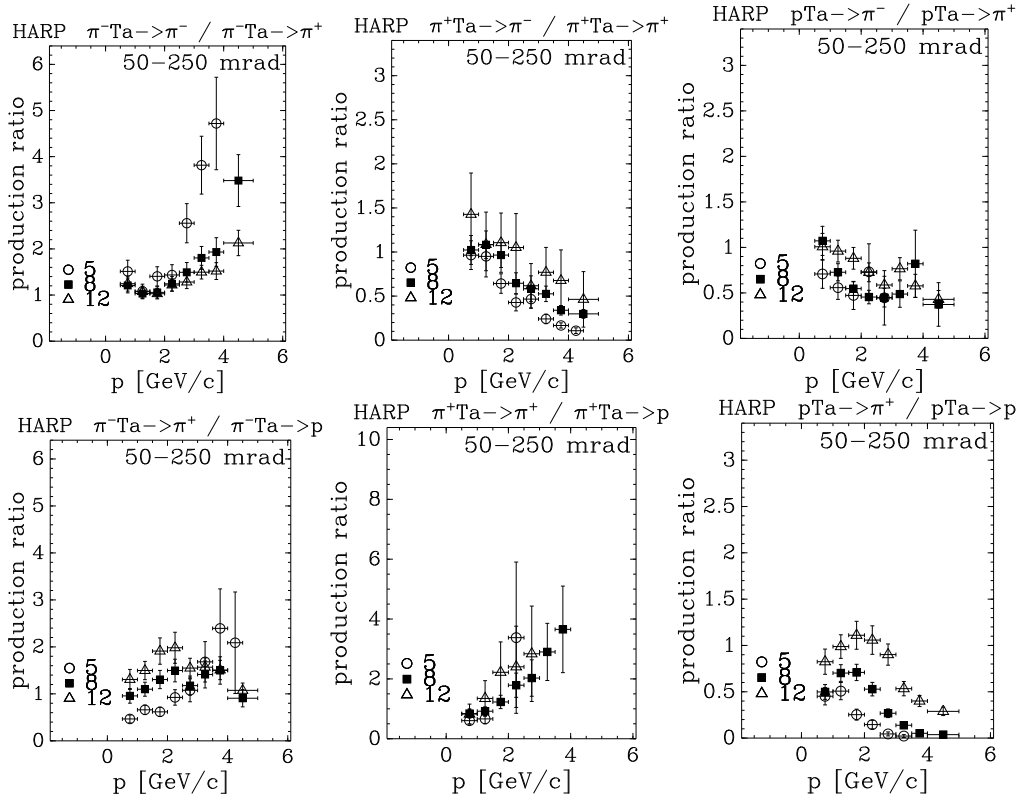


FIG. 8: Particle production ratios on a Ta target at 5, 8, 12 GeV/c. Top panels: π^-/π^+ ratio with incident π^- , π^+ and p; bottom panels: π^+/p ratio with incident π^- , π^+ and p.

A. Comparison with Monte Carlo generators.

In the following we will show only some comparisons with two widely used Monte Carlo simulation packages: MARS [31] and GEANT4 [28]⁷, using different generator models. The comparison will be shown for a limited set of plots and only for the Be and Ta targets, as examples of a light and a heavy target. In both generators, no single model is applicable to all energies and a transition between low energy models and high energy models, at about 5–10 GeV, is needed.

The lack of hadron nuclei collisions data with small errors (both statistics and systematics) on an extended set of thin targets has been, up to now, an obstacle for a serious tuning of these models. Dedicated simulations, such as GiBUU [32], may also profit from the availability of our data.

At intermediate energies (up to 5–10 GeV), GEANT4 uses two types of intra-nuclear cascade models: the Bertini model [33, 34] (valid up to ~ 10 GeV) and the binary model [35] (valid up to ~ 3 GeV). Both models treat the target nucleus in detail, taking into account density variations and tracking in the nuclear field. The binary model is based on hadron collisions with nucleons, giving resonances that decay according to their quantum numbers. The Bertini model is based on the cascade code reported in [36] and hadron collisions are assumed to proceed according to free-space partial cross sections and final state distributions measured for the incident particle types. Details of the nuclear density and the Pauli blocking are then taken into account.

At higher energies, instead, two parton string models, the quark-gluon string (QGS) model [33, 37] and the Fritiof (FTP) model [37] are used, in addition to a High Energy Parametrized model (HEP) derived from the high energy part of the GHEISHA code used inside GEANT3 [38]. The parametrized models of GEANT4 (HEP and LEP) are intended to be fast, but conserve energy and momentum on average and not event-by-event.

A realistic GEANT4 simulation is built by combining models and physics processes into what is called a “physics list”, that is included in the standard GEANT4 Toolkit release. Each physics list corresponds to a collection of models suitable for a given user problem.

As examples, the QGSP physics list is based on

the QGS model, the pre-compound nucleus model and some of the Low Energy Parametrized (LEP) model⁸, while the LHEP physics list [39] is based on the parametrized LEP model and HEP models. Currently the most widely used physics list in LHC experiments is the so-called QGSP-Bert physics list, see reference [40] for details.

The MARS code system [31] uses as basic model an inclusive approach multi-particle production originated by R. Feynman. Above 5 GeV phenomenological particle production models are used, while below 5 GeV a cascade-exciton model [41] combined with the Fermi break-up model, the coalescence model, an evaporation model and a multi-fragmentation extension are used instead.

The comparison, just outlined in our paper, between data and models is reasonable, but some discrepancies are evident for some models especially at lower energies and small angles. Discrepancies up to a factor of three are seen.

The full set of HARP data, taken with targets spanning the full periodic table of elements, with small total errors and full coverage of the solid angle in a single detector may help the validation of models used in hadronic simulations in the difficult energy range between 3 and 15 GeV/ c of incident momentum, as done e.g. in reference [32] for charged pion production.

⁷ The GEANT4 version used is 9.2p01

⁸ Also this model, at low energy, has its root in the GHEISHA code inside GEANT3.

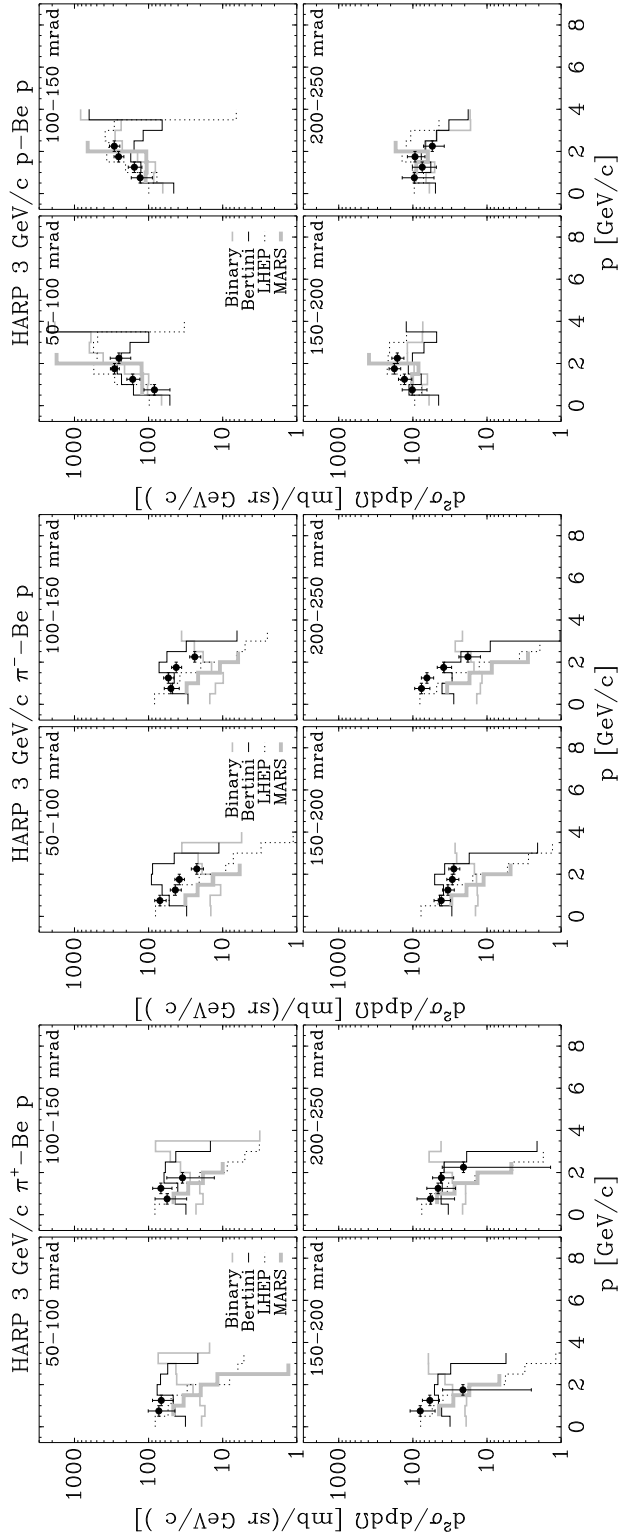


FIG. 9: Comparison of HARP double-differential proton cross sections for p-Be, π^- -Be, π^+ -Be interactions at 3 GeV/c with GEANT4 and MARS MC predictions, using several generator models (see text for details).

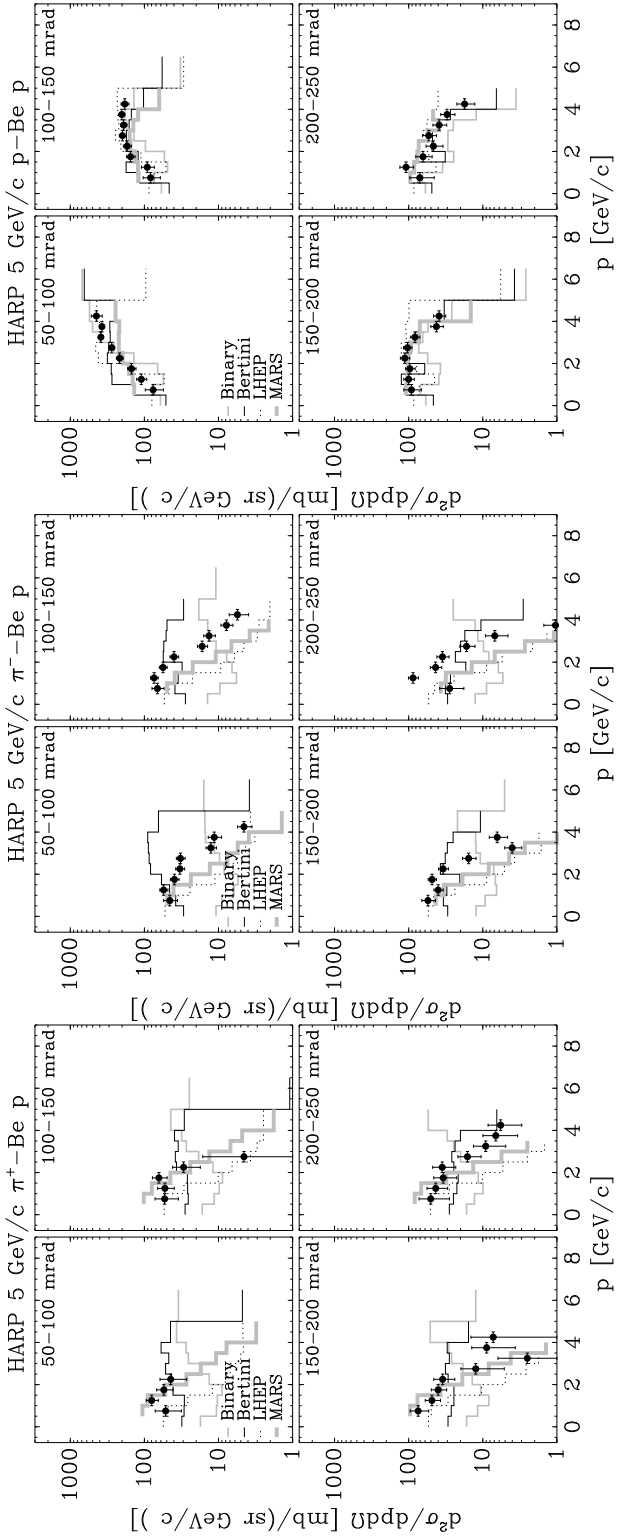


FIG. 10: Comparison of HARP double-differential proton cross sections for p-Be, π^- -Be, π^+ -Be interactions at 5 GeV/c with GEANT4 and MARS MC predictions, using several generator models (see text for details).

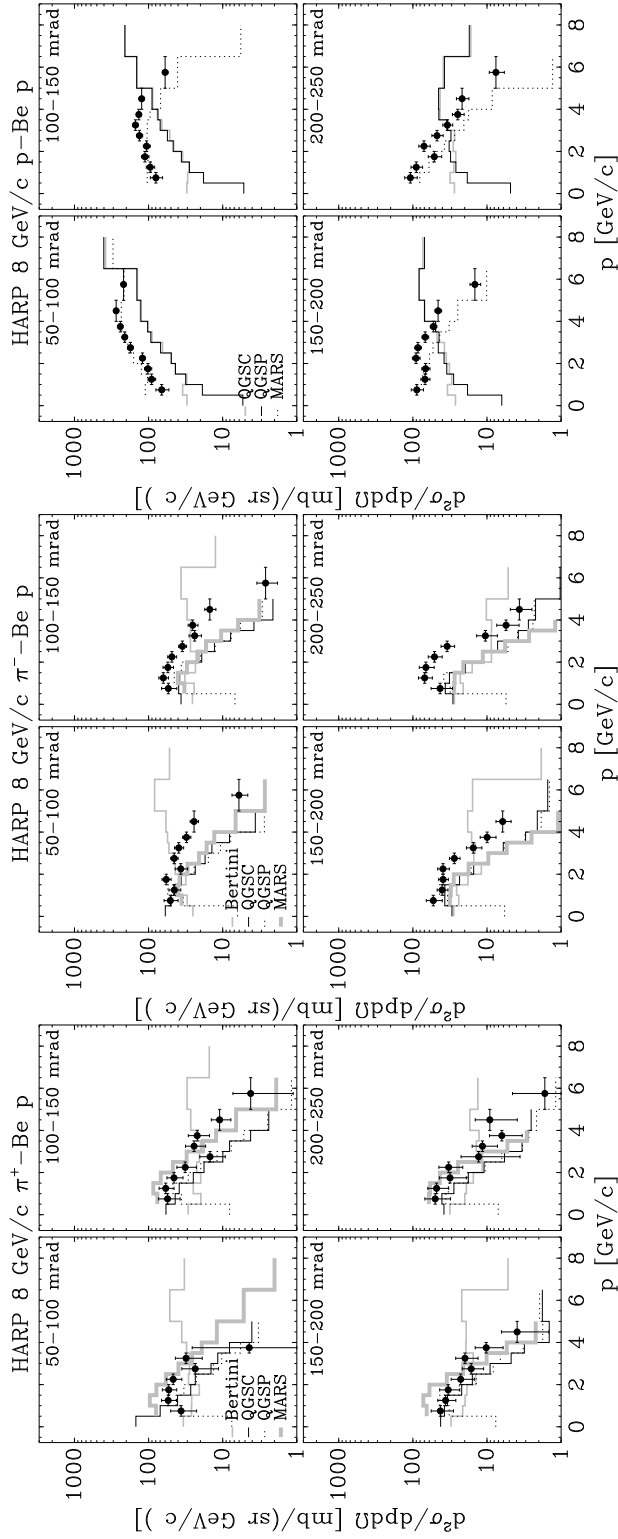


FIG. 11: Comparison of HARP double-differential proton cross sections for p-Be, π^- -Be, π^+ -Be interactions at 8 GeV/c with GEANT4 and MARS MC predictions, using several generator models (see text for details).

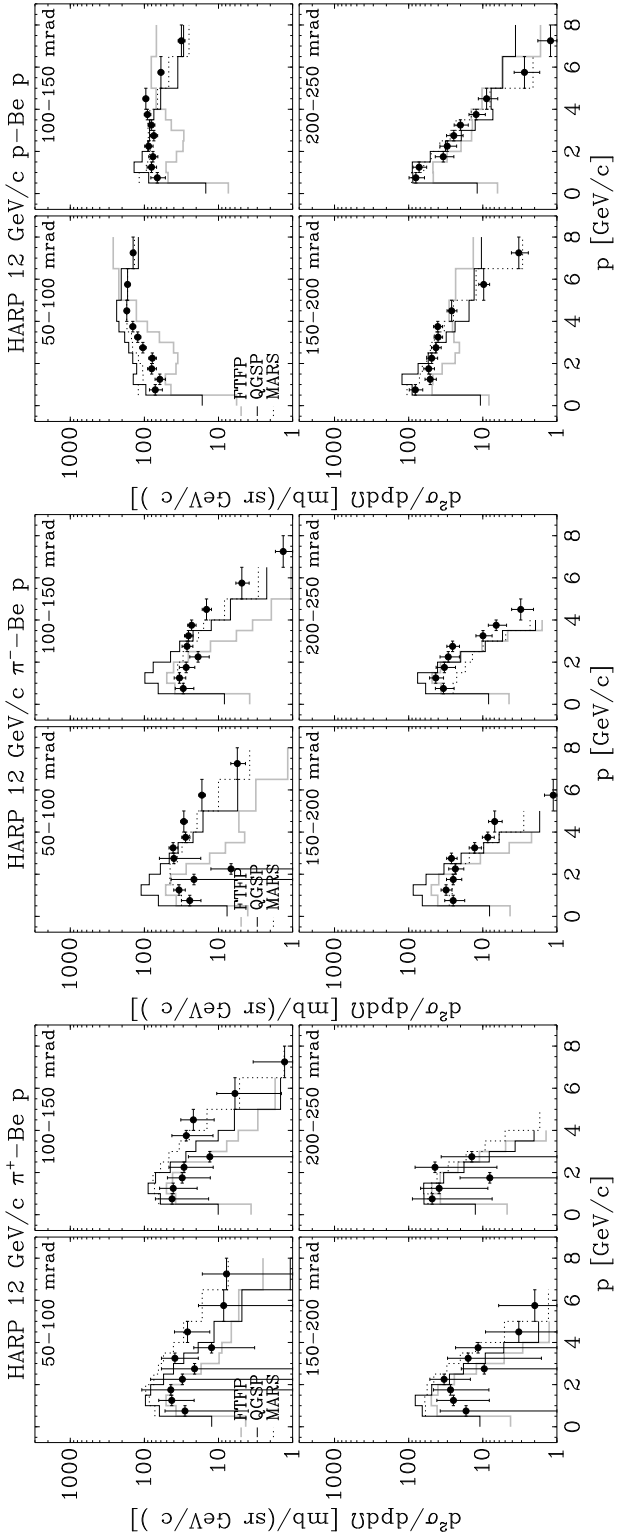


FIG. 12: Comparison of HARP double-differential proton cross sections for p-Be, π^- -Be, π^+ -Be interactions at 12 GeV/c with GEANT4 and MARS MC predictions, using several generator models (see text for details).

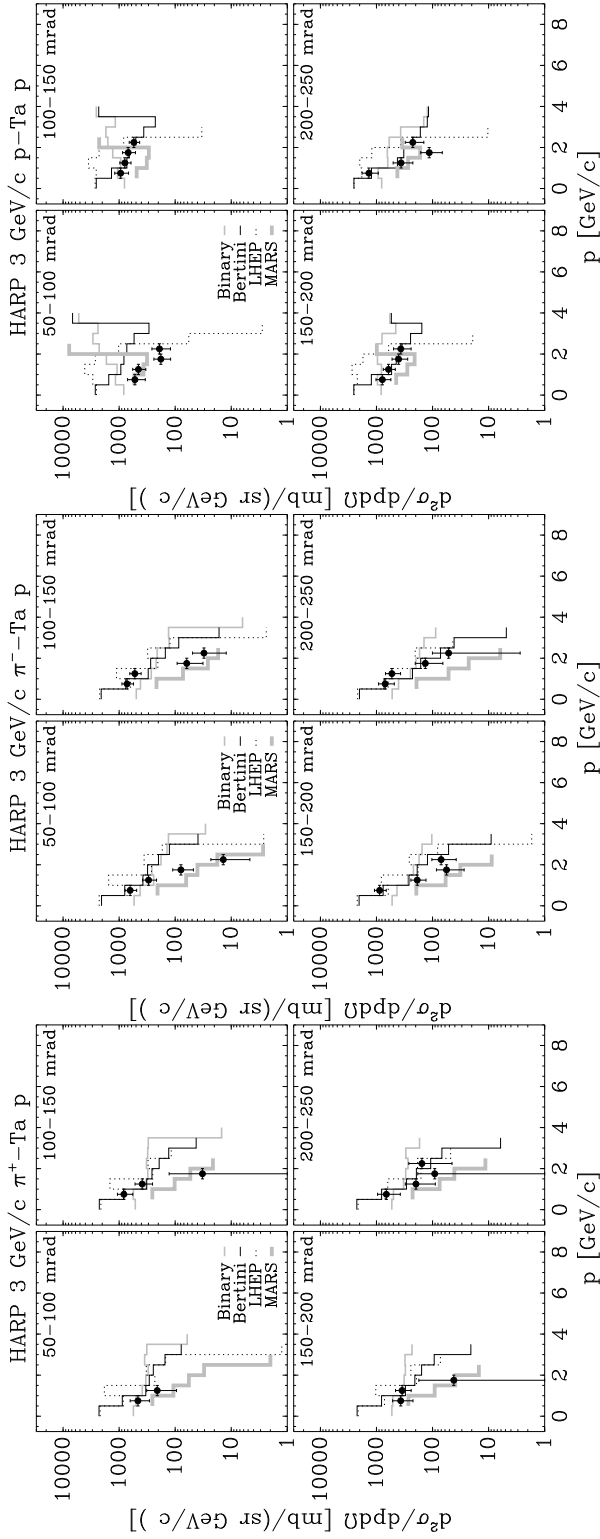


FIG. 13: Comparison of HARP double-differential proton cross sections for p -Ta, π^- -Ta, π^+ -Ta interactions at 3 GeV/c with GEANT4 and MARS MC predictions, using several generator models (see text for details).

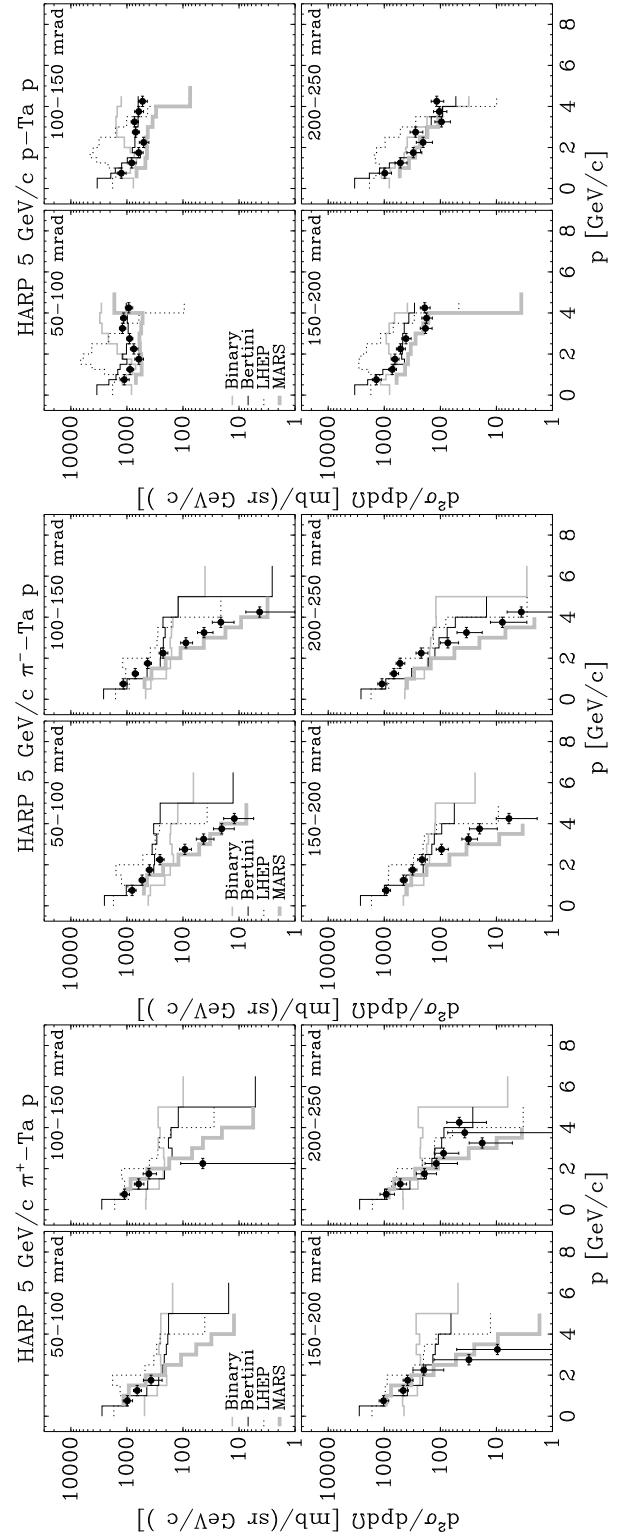


FIG. 14: Comparison of HARP double-differential proton cross sections for p -Ta, π^- -Ta, π^+ -Ta interactions at 5 GeV/c with GEANT4 and MARS MC predictions, using several generator models (see text for details).

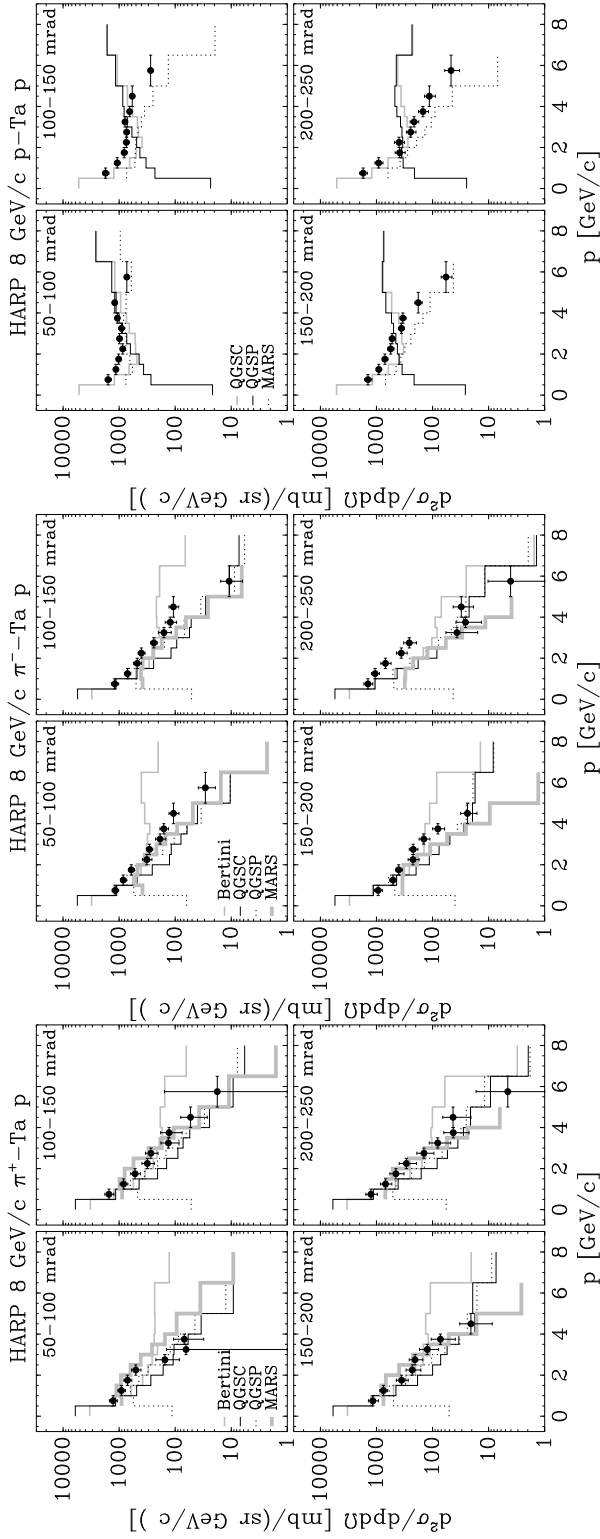


FIG. 15: Comparison of HARP double-differential proton cross sections for $p\text{-Ta}$, $\pi^+\text{-Ta}$, $\pi^-\text{-Ta}$ interactions at 8 GeV/c with GEANT4 and MARS MC predictions, using several generator models (see text for details).

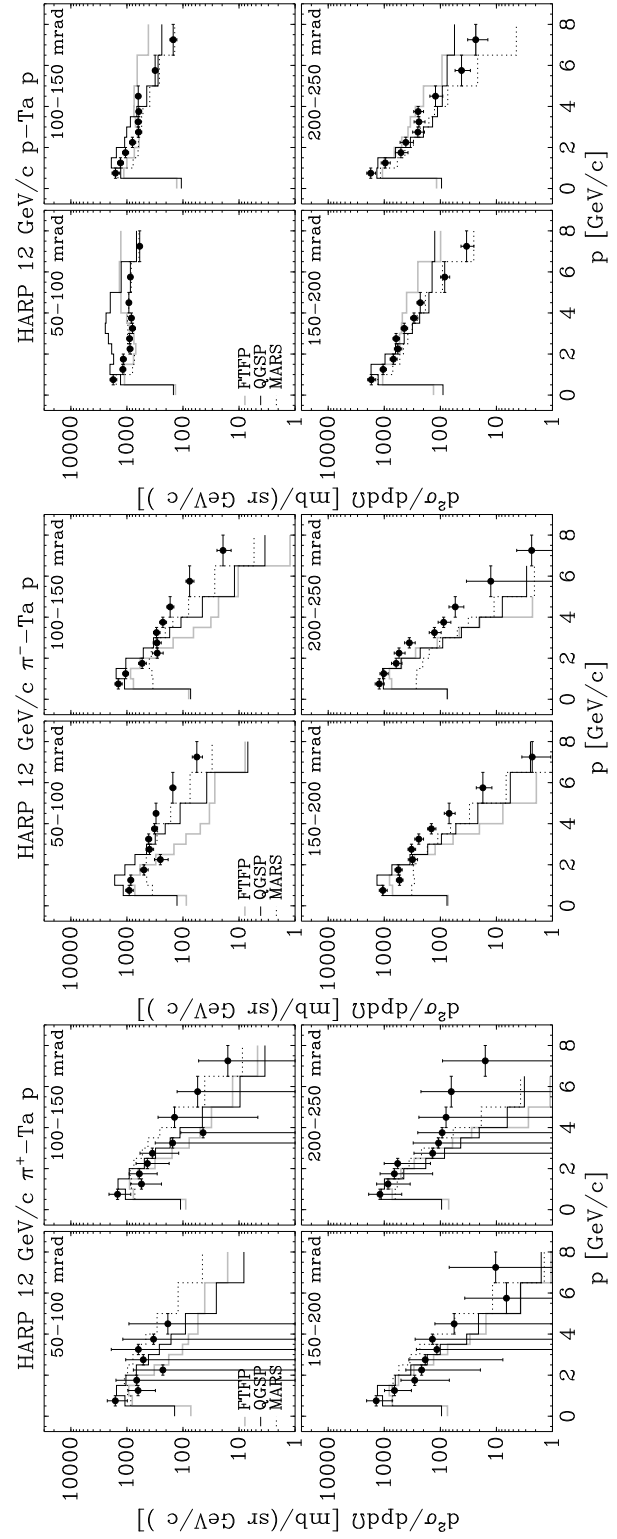


FIG. 16: Comparison of HARP double-differential proton cross sections for $p\text{-Ta}$, $\pi^+\text{-Ta}$, $\pi^-\text{-Ta}$ interactions at 12 GeV/c with GEANT4 and MARS MC predictions, using several generator models (see text for details).

IV. SUMMARY AND CONCLUSIONS

In this paper we report our results on double-differential cross sections for the forward production of protons in the kinematic range $0.5 \text{ GeV}/c \leq p_\pi < 8 \text{ GeV}/c$ and $0.05 \text{ rad} \leq \theta_\pi < 0.25 \text{ rad}$ from the collisions of protons and charged pions of 3, 5, 8 and 12 GeV/c on beryllium, carbon, aluminium, copper, tin, tantalum and lead targets of 5% λ_1 thickness.

The proton yield averaged over different momentum and angular ranges increases smoothly with the atomic number A of the target and with the energy of the incoming beam.

Comparisons with GEANT4 and MARS generators are presented.

We stress that the HARP data presented here are the first precision measurements of forward proton production in this kinematic region and may have a major impact on the tuning of Monte Carlo generators.

Acknowledgments

We gratefully acknowledge the help and support of the PS beam staff and of the numerous technical collaborators who contributed to the detector design, construction, commissioning and operation. In particular, we would like to thank G. Barichello, R. Brocard, K. Burin, V. Carassiti, F. Chignoli, D. Conventi, G. Decreuse, M. Delattre, C. Detraz, A. Domeniconi, M. Dwuznik, F. Evangelisti, B. Friend, A. Iacifano, I. Krasin, D. Lacroix, J.-C. Legrand, M. Lobello, M. Lollo, J. Loquet, F. Marinilli, R. Mazza, J. Mulon, L. Musa, R. Nicholson,

A. Pepato, P. Petev, X. Pons, I. Rusinov, M. Scandurra, E. Usenko, R. van der Vlugt, for their support in the construction of the detector and P. Dini for his contribution to Monte Carlo production. The collaboration acknowledges the major contributions and advice of M. Baldo-Ceolin, L. Linssen, M.T. Muciaccia and A. Pullia during the construction of the experiment. The collaboration is indebted to V. Ableev, F. Bergsma, P. Binko, E. Boter, M. Calvi, C. Cavion, M. Chizov, A. Chukanov, A. DeSanto, A. DeMin, M. Doucet, D. Düllmann, V. Ermilova, W. Flegel, Y. Hayato, A. Ichikawa, O. Klimov, T. Kobayashi, D. Kustov, M. Laveder, M. Mass, H. Meinhard, A. Menegolli, T. Nakaya, K. Nishikawa, M. Paganoni, F. Paleari, M. Pasquali, M. Placentino, V. Serdiouk, S. Simone, P.J. Soler, S. Troquereau, S. Ueda, A. Valassi and R. Veenhof for their contributions to the experiment.

We acknowledge the contributions of V. Amosov, G. Chelkov, D. Dedovich, F. Dydak, M. Gostkin, A. Guskov, D. Khartchenko, V. Korshchev, Z. Kroumchtein, I. Nefedov, A. Semak, J. Wotschack, V. Zaets and A. Zhemchugov to the work described in this paper.

The experiment was made possible by grants from the Institut Interuniversitaire des Sciences Nucléaires and the Interuniversitair Instituut voor Kernwetenschappen (Belgium), Ministerio de Educacion y Ciencia, Grant FPA2003-06921-c02-02 and Generalitat Valenciana, grant GV00-054-1, CERN (Geneva, Switzerland), the German Bundesministerium für Bildung und Forschung (Germany), the Istituto Nazionale di Fisica Nucleare (Italy), INR RAS (Moscow), the Russian Foundation for Basic Research (grant 08-02-00018), the Bulgarian National Science Fund (contract VU-F-205/2006) and the Particle Physics and Astronomy Research Council (UK). We gratefully acknowledge their support.

-
- [1] M.G. Catanesi *et al.*, HARP Collaboration, “Proposal to study hadron production for the neutrino factory and for the atmospheric neutrino flux”, CERN-SPSC/99-35 (1999).
- [2] A. Blondel *et al.*, CERN-2004-002, ECFA/04/230; M. M.Alsharoa *et al.*, Phys. Rev. ST. Accel. Beams 6, 081001 (2003); M. Apollonio *et al.*, “Oscillation Physics with a Neutrino Factory”, CERN TH2002-208, [arXiv:hep-ph/0210192].
- [3] G. Battistoni, Nucl. Phys. Proc. Suppl. **B100** (2001) 101.
- [4] T. Stanev, Rapporteur’s talk at the 26th Int. Cosmic Ray Conference (Salt Lake City, Utah, USA; eds. B.L. Dingus *et al.*, AIP Conf. Proceedings 516, (2000) 247).
- [5] T.K. Gaisser, Nucl. Phys. Proc. Suppl. **B87** (2000) 145.
- [6] R. Engel, T.K. Gaisser and T. Stanev, Phys. Lett. **B472** (2000) 113.
- [7] M. Bonesini and A. Guglielmi, Phys. Rep. **433** (2006) 66.
- [8] M.H. Ahn *et al.*, K2K Collaboration, Phys. Rev. Lett. **90** (2003) 041801.
- [9] M. H. Ahn *et al.*, K2K Collaboration, Phys. Rev. **D74** (2006) 072003, arXiv:hep-ex/0606032.
- [10] A. A. Aguilar-Arevalo, The MiniBooNE Collaboration, “A Search for Electron Neutrino Appearance at the $\Delta m^2 \sim 1 \text{ eV}^2$ Scale“, arXiv:0704.1500.

- E. Church *et al.*, BooNe Collaboration, “A proposal for an experiment to measure muon-neutrino \rightarrow electron-neutrino oscillations and muon-neutrino disappearance at the Fermilab Booster: BooNE”, FERMILAB-PROPOSAL-0898, (1997).
- [11] A. A. Aguilar-Arevalo *et al.*, SciBooNE Collaboration, “Bringing the SciBar detector to the Booster neutrino beam,” FERMILAB-PROPOSAL-0954, (2006), arXiv:hep-ex/0601022.
- [12] G. Ambrosini *et al.*, NA56 Collaboration, Eur. Phys. J. C **10** (1999) 605;
G. Ambrosini *et al.*, NA56 Collaboration, Phys. Lett. B **420** (1998) 225;
G. Ambrosini *et al.*, NA56 Collaboration, Phys. Lett. B **425** (1998) 208.
- [13] H.W. Atherton, CERN 80-07, August 1980.
- [14] M. G. Catanesi *et al.*, HARP Collaboration, Nucl. Phys. **B732** (2006) 1 arXiv:hep-ex/0510039.
- [15] M. G. Catanesi *et al.*, HARP Collaboration, Eur. Phys. J. **C52** (2007) 29, arXiv:hep-ex/0702024.
- [16] M. G. Catanesi *et al.*, HARP Collaboration, Astroparticle Physics **29** (2008) 257, arXiv:0802.0657 [astro-ph].
- [17] M. G. Catanesi *et al.*, HARP Collaboration, Astroparticle Physics **30** (2008) 124, arXiv:0807.1025 [hep-ex].
- [18] M. Apollonio *et al.*, HARP Collaboration, Phys. Rev. **C80** (2009) 035208, arXiv:0907.3857 [hep-ex].
- [19] M. Apollonio *et al.*, HARP Collaboration, Nucl. Phys. **A821** (2009) 118, arXiv:0902.2105 [hep-ex].
- [20] M.G. Catanesi *et al.*, HARP Collaboration, Phys. Rev. **C77** (2008) 055207, arXiv:0805.2871 [hep-ex].
- [21] M. Apollonio *et al.*, HARP Collaboration, Phys. Rev. **C80** (2009) 065207, arXiv:0907.1428 [hep-ex].
- [22] M.G. Catanesi *et al.*, HARP Collaboration, Nucl. Instrum. Meth. **A571** (2007) 527; **A571** (2007) 564.
- [23] M. Anfreville *et al.*, Nucl. Instrum. Meth. **A481** (2002) 339.
- [24] M. Baldo-Ceolin *et al.*, Nucl. Instrum. Meth. **A532** (2004) 548;
M. Bonesini *et al.*, IEEE Trans. Nucl. Sci. NS-50 (2003) 1053.
- [25] M. G. Catanesi *et al.*, HARP Collaboration, Nucl. Instrum. Meth. A **572** (2007) 899.
- [26] L. Durieu, A. Mueller and M. Martini, PAC-2001-TPAH142 IEEE Particle Accelerator Conference (PAC2001), Chicago, Illinois, 18-22 Jun 2001;
L. Durieu *et al.*, Proceedings of PAC’97, Vancouver, (1997);
L. Durieu, O. Fernando, CERN PS/PA Note 96-38.
- [27] K. Pretzl *et al.*, Invited talk at the “International Symposium on Strangeness and Quark Matter”, Crete, (1999) 230.
- [28] S. Agostinelli *et al.* [GEANT4 Collaboration], Nucl. Instrum. Meth. A **506** (2003) 250.
- [29] G. D’Agostini, DESY 94-099, ISSN 0418-9833, 1994.
G. D’Agostini, Nucl. Instrum. Meth. A **362** (1995) 487.
- [30] A. Grossheim, “Particle production yields induced by multi-GeV protons on nuclear targets”, Ph.D. thesis, University of Dortmund, Germany, 2003, CERN-THESIS-2004-010.
- [31] N.V. Mokhov, S.I. Striganov, “MARS overview”, FERMILAB-CONF-07-008-AD, 2007.
- [32] K. Gallmeister, U. Mosel, Nucl. Phys. A **826** (2009) 151, arXiv:0901.1770 [hep-ex].
- [33] D.H. Wright *et al.*, AIP Conf. Proc. 896 (2007) 11.
- [34] A. Heikkinen *et al.*, arXiv:nucl-th/0306008.
- [35] G. Folger, V. Ivanchenko and H.P. Wellisch, Eur. Phys. J. A21 (2004) 407.
- [36] H.W. Bertini, P. Guthrie, Nucl. Phys. **A169** (1971) 670.
- [37] G. Folger and H.P. Wellisch, arXiv:nucl-th/0306007.
- [38] H. Fesefeld, Technical report PITHA 85-02, Aachen, 1985.
- [39] D.H. Wright *et al.*, AIP Conf. Proc. 867 (2006) 479.
- [40] J. Apostolakis *et al.*, J. Phys. Conf. Ser. 160 (2009) 012073.
- [41] S.G. Mashnik *et al.*, LANL report LA-UR-05-7321, 2005.

Appendix A: Cross-section data

The following tables report the measured differential cross-section for forward proton production in interactions of 3, 5, 8 and 12 GeV/ c momentum charged pions or protons on different types of nuclear targets. The data are presented in the kinematic range of $0.5 \text{ GeV}/c \leq p_\pi < 8 \text{ GeV}/c$ and $0.05 \text{ rad} \leq \theta_\pi < 0.25 \text{ rad}$. The overall normalization uncertainty ($\leq 2\%$) is not included in the reported errors.

TABLE II: HARP results for the double-differential p production cross-section in the laboratory system, $d^2\sigma^p/(dpd\Omega)$, for π^- -Be interactions at 3,5,8,12 GeV/c. Each row refers to a different ($p_{\min} \leq p < p_{\max}, \theta_{\min} \leq \theta < \theta_{\max}$) bin, where p and θ are the outgoing proton momentum and polar angle, respectively. The central value as well as the square-root of the diagonal elements of the covariance matrix are given.

θ_{\min} (rad)	θ_{\max} (rad)	p_{\min} (GeV/c)	p_{\max} (GeV/c)	$d^2\sigma^p/(dpd\Omega)$ (barn/(sr GeV/c))			
				3 GeV/c	5 GeV/c	8 GeV/c	12 GeV/c
0.050	0.100	0.50	1.00	0.070±0.012	0.045±0.010	0.051±0.011	0.024±0.007
			1.00	0.044±0.007	0.055±0.007	0.045±0.008	0.034±0.006
		1.50	2.00	0.039±0.006	0.039±0.005	0.058±0.008	0.021±0.022
			2.00	0.022±0.004	0.033±0.005	0.037±0.007	0.007±0.006
		2.50	3.00	±	0.033±0.004	0.045±0.005	0.04±0.02
			3.00	±	0.013±0.002	0.039±0.006	0.041±0.006
		3.50	4.00	±	0.011±0.002	0.031±0.004	0.028±0.004
			4.00	±	0.005±0.001	0.024±0.003	0.029±0.003
		5.00	6.50	±	±	0.006±0.001	0.017±0.002
			6.50	±	±	±	0.006±0.001
0.100	0.150	0.50	1.00	0.050±0.011	0.067±0.012	0.054±0.013	0.030±0.008
			1.00	0.054±0.008	0.074±0.009	0.063±0.009	0.034±0.006
		1.50	2.00	0.042±0.007	0.056±0.007	0.055±0.009	0.027±0.006
			2.00	0.024±0.004	0.040±0.005	0.049±0.007	0.019±0.006
		2.50	3.00	±	0.017±0.003	0.035±0.004	0.027±0.004
			3.00	±	0.013±0.002	0.024±0.005	0.025±0.003
		3.50	4.00	±	0.008±0.001	0.025±0.004	0.023±0.003
			4.00	±	0.006±0.002	0.015±0.003	0.015±0.002
		5.00	6.50	±	±	0.003±0.001	0.005±0.001
			6.50	±	±	±	±
0.150	0.200	0.50	1.00	0.041±0.010	0.055±0.012	0.053±0.013	0.025±0.008
			1.00	0.034±0.006	0.040±0.006	0.040±0.007	0.031±0.005
		1.50	2.00	0.029±0.005	0.048±0.006	0.039±0.006	0.025±0.006
			2.00	0.028±0.005	0.034±0.005	0.039±0.007	0.023±0.005
		2.50	3.00	±	0.016±0.003	0.028±0.005	0.026±0.004
			3.00	±	0.004±0.001	0.015±0.004	0.013±0.002
		3.50	4.00	±	0.006±0.002	0.010±0.002	0.009±0.002
			4.00	±	0.001±0.001	0.006±0.001	0.007±0.001
		5.00	6.50	±	±	±	±
			6.50	±	±	±	±
0.200	0.250	0.50	1.00	0.08±0.02	0.028±0.010	0.043±0.014	0.034±0.010
			1.00	0.065±0.012	0.087±0.013	0.069±0.015	0.043±0.009
		1.50	2.00	0.038±0.008	0.043±0.008	0.07±0.02	0.033±0.010
			2.00	0.018±0.006	0.035±0.007	0.051±0.011	0.029±0.009
		2.50	3.00	±	0.017±0.004	0.034±0.007	0.026±0.005
			3.00	±	0.007±0.002	0.011±0.003	0.010±0.002
		3.50	4.00	±	±	0.006±0.002	0.007±0.002
			4.00	±	±	0.004±0.001	0.003±0.001
		5.00	6.50	±	±	0.000±0.001	±
			6.50	±	±	±	±

TABLE III: HARP results for the double-differential p production cross-section in the laboratory system, $d^2\sigma^p/(dpd\Omega)$, for π^+ -Be interactions at 3,5,8,8.9 GeV/c. Each row refers to a different ($p_{\min} \leq p < p_{\max}, \theta_{\min} \leq \theta < \theta_{\max}$) bin, where p and θ are the outgoing proton momentum and polar angle, respectively. The central value as well as the square-root of the diagonal elements of the covariance matrix are given.

θ_{\min} (rad)	θ_{\max} (rad)	p_{\min} (GeV/c)	p_{\max} (GeV/c)	$d^2\sigma^p/(dpd\Omega)$ (barn/(sr GeV/c))			
				3 GeV/c	5 GeV/c	8 GeV/c	8.9 GeV/c
0.050	0.100	0.50	1.00	0.07±0.03	0.05±0.02	0.036±0.014	0.042±0.012
			1.00	0.07±0.02	0.080±0.015	0.054±0.012	0.061±0.009
		1.50	2.00	±0.000	0.055±0.014	0.053±0.012	0.053±0.009
			2.00	±0.02	0.04±0.02	0.047±0.011	0.047±0.006
		2.50	3.00	±	±	0.024±0.012	0.047±0.007
			3.00	±	±	0.031±0.012	0.042±0.006
		3.50	4.00	±	±	0.004±0.021	0.048±0.005
			4.00	±	±	±	0.042±0.004
		5.00	±	±	±	0.020±0.003	
0.100	0.150	0.50	1.00	0.06±0.03	0.05±0.02	0.06±0.02	0.049±0.015
			1.00	0.07±0.02	0.053±0.013	0.059±0.013	0.047±0.009
		1.50	2.00	0.03±0.02	0.064±0.014	0.045±0.011	0.053±0.007
			2.00	±	0.030±0.012	0.032±0.009	0.045±0.007
		2.50	3.00	±	0.005±0.012	0.015±0.006	0.044±0.006
			3.00	±	±	0.024±0.007	0.037±0.005
		3.50	4.00	±	±	0.022±0.007	0.035±0.004
			4.00	±	±	0.011±0.003	0.024±0.003
		5.00	±	±	0.004±0.003	0.007±0.001	
0.150	0.200	0.50	1.00	0.08±0.03	0.07±0.02	0.042±0.014	0.047±0.011
			1.00	0.06±0.02	0.049±0.011	0.036±0.010	0.054±0.006
		1.50	2.00	0.02±0.02	0.040±0.009	0.033±0.010	0.028±0.006
			2.00	±	0.035±0.011	0.023±0.008	0.031±0.007
		2.50	3.00	±	0.012±0.007	0.016±0.005	0.024±0.005
			3.00	±	0.003±0.004	0.020±0.007	0.012±0.004
		3.50	4.00	±	0.009±0.005	0.010±0.004	0.011±0.003
			4.00	±	0.007±0.007	0.004±0.002	0.009±0.002
		5.00	±	±	0.000±0.001	±	
0.200	0.250	0.50	1.00	0.06±0.03	0.05±0.02	0.05±0.02	0.042±0.013
			1.00	0.05±0.02	0.043±0.013	0.05±0.02	0.048±0.009
		1.50	2.00	0.041±0.013	0.034±0.012	0.031±0.013	0.038±0.007
			2.00	0.02±0.02	0.035±0.012	0.033±0.012	0.028±0.006
		2.50	3.00	±	0.016±0.006	0.013±0.009	0.017±0.004
			3.00	±	0.009±0.004	0.012±0.004	0.009±0.002
		3.50	4.00	±	0.007±0.003	0.006±0.003	0.006±0.002
			4.00	±	0.006±0.003	0.009±0.005	0.003±0.002
		5.00	±	±	0.002±0.003	0.001±0.001	

TABLE IV: HARP results for the double-differential p production cross-section in the laboratory system, $d^2\sigma^p/(dpd\Omega)$, for p-Be interactions at 3,5,8,8.9,12 GeV/c. Each row refers to a different ($p_{\min} \leq p < p_{\max}, \theta_{\min} \leq \theta < \theta_{\max}$) bin, where p and θ are the outgoing proton momentum and polar angle, respectively. The central value as well as the square-root of the diagonal elements of the covariance matrix are given.

θ_{\min} (rad)	θ_{\max} (rad)	p_{\min} (GeV/c)	p_{\max} (GeV/c)	$d^2\sigma^p/(dpd\Omega)$ (barn/(sr GeV/c))				
				3 GeV/c	5 GeV/c	8 GeV/c	8.9 GeV/c	12 GeV/c
0.050	0.100	0.50	1.00	0.08±0.03	0.08±0.02	0.067±0.013	0.079±0.013	0.071±0.014
			1.00	0.16±0.03	0.11±0.02	0.091±0.011	0.080±0.010	0.062±0.010
		1.50	2.00	0.29±0.04	0.15±0.02	0.102±0.011	0.100±0.010	0.080±0.011
			2.00	0.25±0.08	0.22±0.02	0.121±0.010	0.116±0.010	0.078±0.009
		2.50	3.00	±	0.28±0.02	0.176±0.015	0.134±0.010	0.105±0.010
			3.00	±	0.39±0.03	0.210±0.015	0.170±0.013	0.123±0.011
		3.50	4.00	±	0.37±0.03	0.24±0.02	0.197±0.013	0.143±0.012
			4.00	±	0.44±0.07	0.274±0.013	0.223±0.010	0.173±0.010
		5.00	6.50	±	±	0.218±0.008	0.206±0.008	0.169±0.008
			6.50	±	±	±	±	0.142±0.006
0.100	0.150	0.50	1.00	0.13±0.04	0.08±0.02	0.080±0.015	0.082±0.014	0.067±0.015
			1.00	0.16±0.03	0.09±0.02	0.095±0.012	0.093±0.011	0.080±0.012
		1.50	2.00	0.25±0.04	0.15±0.02	0.112±0.013	0.092±0.010	0.077±0.011
			2.00	0.29±0.05	0.17±0.02	0.106±0.011	0.092±0.009	0.088±0.011
		2.50	3.00	±	0.20±0.02	0.133±0.013	0.113±0.011	0.075±0.008
			3.00	±	0.19±0.02	0.151±0.012	0.121±0.009	0.081±0.008
		3.50	4.00	±	0.20±0.02	0.135±0.010	0.112±0.008	0.091±0.009
			4.00	±	0.18±0.02	0.124±0.010	0.109±0.008	0.096±0.008
		5.00	6.50	±	±	0.060±0.005	0.058±0.005	0.060±0.005
			6.50	±	±	±	±	0.032±0.003
0.150	0.200	0.50	1.00	0.10±0.04	0.09±0.02	0.09±0.02	0.078±0.014	0.08±0.02
			1.00	0.13±0.03	0.10±0.02	0.068±0.009	0.067±0.007	0.051±0.009
		1.50	2.00	0.18±0.03	0.10±0.01	0.067±0.009	0.060±0.008	0.054±0.009
			2.00	0.16±0.03	0.11±0.02	0.091±0.011	0.072±0.008	0.049±0.008
		2.50	3.00	±	0.104±0.014	0.085±0.009	0.058±0.006	0.043±0.006
			3.00	±	0.082±0.012	0.068±0.007	0.062±0.006	0.040±0.005
		3.50	4.00	±	0.042±0.008	0.053±0.005	0.047±0.005	0.040±0.006
			4.00	±	0.039±0.007	0.046±0.005	0.033±0.003	0.026±0.004
		5.00	6.50	±	±	0.015±0.002	0.014±0.002	0.010±0.002
			6.50	±	±	±	±	0.003±0.001
0.200	0.250	0.50	1.00	0.10±0.04	0.07±0.03	0.11±0.02	0.083±0.015	0.08±0.02
			1.00	0.07±0.03	0.11±0.02	0.09±0.02	0.071±0.010	0.07±0.02
		1.50	2.00	0.09±0.02	0.06±0.02	0.051±0.011	0.056±0.009	0.034±0.010
			2.00	0.05±0.02	0.046±0.012	0.071±0.012	0.050±0.007	0.030±0.008
		2.50	3.00	±	0.054±0.011	0.047±0.008	0.040±0.006	0.025±0.006
			3.00	±	0.039±0.008	0.034±0.005	0.022±0.003	0.020±0.004
		3.50	4.00	±	0.030±0.007	0.025±0.004	0.017±0.003	0.012±0.003
			4.00	±	0.018±0.005	0.022±0.004	0.018±0.003	0.009±0.003
		5.00	6.50	±	±	0.008±0.002	0.006±0.001	0.003±0.001
			6.50	±	±	±	±	0.001±0.001

TABLE V: HARP results for the double-differential p production cross-section in the laboratory system, $d^2\sigma^p/(dpd\Omega)$, for π^- -C interactions at 3,5,8,12 GeV/c. Each row refers to a different ($p_{\min} \leq p < p_{\max}, \theta_{\min} \leq \theta < \theta_{\max}$) bin, where p and θ are the outgoing proton momentum and polar angle, respectively. The central value as well as the square-root of the diagonal elements of the covariance matrix are given.

θ_{\min} (rad)	θ_{\max} (rad)	p_{\min} (GeV/c)	p_{\max} (GeV/c)	$d^2\sigma^p/(dpd\Omega)$ (barn/(sr GeV/c))			
				3 GeV/c	5 GeV/c	8 GeV/c	12 GeV/c
0.050	0.100	0.50	1.00	0.11±0.02	0.08±0.02	0.08±0.02	0.05±0.02
			1.00	0.056±0.014	0.068±0.011	0.057±0.012	0.060±0.013
		1.50	2.00	0.054±0.011	0.069±0.010	0.077±0.012	0.05±0.03
			2.00	0.031±0.008	0.045±0.007	0.051±0.010	0.005±0.006
		2.50	3.00	±	0.026±0.005	0.052±0.007	0.035±0.011
			3.00	±	0.018±0.005	0.041±0.007	0.056±0.009
		3.50	4.00	±	0.012±0.003	0.043±0.006	0.052±0.007
			4.00	±	0.008±0.003	0.020±0.004	0.055±0.006
		5.00	6.50	±	±	0.007±0.002	0.026±0.004
			6.50	±	±	±	0.011±0.002
0.100	0.150	0.50	1.00	0.08±0.02	0.07±0.02	0.07±0.02	0.05±0.02
			1.00	0.07±0.02	0.077±0.013	0.069±0.012	0.065±0.014
		1.50	2.00	0.071±0.015	0.060±0.010	0.061±0.011	0.036±0.011
			2.00	0.022±0.007	0.047±0.008	0.048±0.008	0.034±0.012
		2.50	3.00	±	0.029±0.006	0.051±0.006	0.036±0.008
			3.00	±	0.011±0.003	0.025±0.006	0.048±0.008
		3.50	4.00	±	0.011±0.003	0.022±0.004	0.047±0.007
			4.00	±	0.005±0.002	0.011±0.003	0.031±0.005
		5.00	6.50	±	±	0.003±0.001	0.009±0.002
			6.50	±	±	±	0.003±0.001
0.150	0.200	0.50	1.00	0.09±0.03	0.08±0.02	0.06±0.02	0.07±0.02
			1.00	0.036±0.010	0.048±0.009	0.044±0.009	0.041±0.010
		1.50	2.00	0.037±0.010	0.060±0.010	0.053±0.008	0.047±0.012
			2.00	0.031±0.009	0.034±0.008	0.048±0.010	0.022±0.008
		2.50	3.00	±	0.021±0.005	0.025±0.005	0.033±0.008
			3.00	±	0.010±0.003	0.021±0.005	0.041±0.009
		3.50	4.00	±	0.003±0.002	0.013±0.003	0.019±0.006
			4.00	±	±	0.007±0.002	0.007±0.002
		5.00	6.50	±	±	±	0.002±0.001
			6.50	±	±	±	±
0.200	0.250	0.50	1.00	0.09±0.03	0.09±0.02	0.06±0.02	0.05±0.02
			1.00	0.11±0.03	0.07±0.02	0.09±0.02	0.06±0.02
		1.50	2.00	0.05±0.02	0.064±0.014	0.06±0.02	0.05±0.02
			2.00	0.034±0.013	0.036±0.009	0.08±0.02	0.04±0.02
		2.50	3.00	±	0.022±0.007	0.035±0.008	0.030±0.010
			3.00	±	0.009±0.004	0.013±0.004	0.015±0.006
		3.50	4.00	±	0.002±0.001	0.010±0.003	0.007±0.003
			4.00	±	±	0.005±0.002	0.004±0.002
		5.00	6.50	±	±	0.001±0.001	±
			6.50	±	±	±	±

TABLE VI: HARP results for the double-differential p production cross-section in the laboratory system, $d^2\sigma^p/(dpd\Omega)$, for π^+ -C interactions at 3,5,8,12 GeV/c. Each row refers to a different ($p_{\min} \leq p < p_{\max}, \theta_{\min} \leq \theta < \theta_{\max}$) bin, where p and θ are the outgoing proton momentum and polar angle, respectively. The central value as well as the square-root of the diagonal elements of the covariance matrix are given.

θ_{\min} (rad)	θ_{\max} (rad)	p_{\min} (GeV/c)	p_{\max} (GeV/c)	$d^2\sigma^p/(dpd\Omega)$ (barn/(sr GeV/c))			
				3 GeV/c	5 GeV/c	8 GeV/c	12 GeV/c
0.050	0.100	0.50	1.00	0.10±0.04	0.07±0.02	0.06±0.02	0.06±0.05
			1.00	0.09±0.03	0.08±0.02	0.07±0.02	0.07±0.04
		1.50	2.00	±	0.07±0.02	0.08±0.02	0.01±0.03
			2.00	±	0.015±0.016	0.063±0.014	0.03±0.08
		2.50	3.00	±	±	0.036±0.013	0.055±0.084
			3.00	±	±	0.002±0.008	0.026±0.039
		3.50	4.00	±	±	0.05±0.02	0.001±0.012
			4.00	±	±	±	±
		5.00	6.50	±	±	±	±
			6.50	±	±	±	0.013±0.008
0.100	0.150	0.50	1.00	0.09±0.04	0.07±0.02	0.06±0.02	0.10±0.07
			1.00	0.10±0.03	0.06±0.01	0.06±0.02	±
		1.50	2.00	0.05±0.03	0.06±0.02	0.06±0.02	0.09±0.05
			2.00	±	0.03±0.02	0.039±0.012	0.03±0.03
		2.50	3.00	±	±	0.040±0.010	0.01±0.02
			3.00	±	±	0.041±0.011	0.024±0.024
		3.50	4.00	±	±	0.018±0.007	±
			4.00	±	±	0.011±0.005	±
		5.00	6.50	±	±	0.006±0.019	±
			6.50	±	±	±	±
0.150	0.200	0.50	1.00	0.10±0.04	0.10±0.02	0.05±0.02	0.09±0.07
			1.00	0.08±0.02	0.070±0.013	0.051±0.014	0.02±0.03
		1.50	2.00	0.018±0.023	0.058±0.011	0.036±0.012	0.05±0.04
			2.00	±	0.029±0.011	0.029±0.010	0.018±0.024
		2.50	3.00	±	0.012±0.008	0.020±0.007	0.014±0.022
			3.00	±	0.005±0.006	0.011±0.005	0.020±0.046
		3.50	4.00	±	0.011±0.007	0.015±0.006	0.005±0.022
			4.00	±	0.006±0.006	0.006±0.003	0.005±0.022
		5.00	6.50	±	±	0.001±0.001	0.001±0.006
			6.50	±	±	±	±
0.200	0.250	0.50	1.00	0.09±0.04	0.07±0.03	0.05±0.02	0.06±0.06
			1.00	0.04±0.02	0.06±0.02	0.09±0.03	0.03±0.06
		1.50	2.00	0.04±0.02	0.036±0.012	0.07±0.02	0.02±0.05
			2.00	0.02±0.02	0.039±0.013	0.028±0.013	0.06±0.09
		2.50	3.00	±	0.024±0.007	0.019±0.008	0.01±0.02
			3.00	±	0.012±0.005	0.024±0.008	0.029±0.058
		3.50	4.00	±	0.007±0.003	0.015±0.005	0.012±0.025
			4.00	±	0.004±0.002	0.014±0.006	0.002±0.011
		5.00	6.50	±	±	0.004±0.003	0.000±0.004
			6.50	±	±	±	0.000±0.005

TABLE VII: HARP results for the double-differential p production cross-section in the laboratory system, $d^2\sigma^p/(dpd\Omega)$, for p -C interactions at 3,5,8,12 GeV/ c . Each row refers to a different ($p_{\min} \leq p < p_{\max}, \theta_{\min} \leq \theta < \theta_{\max}$) bin, where p and θ are the outgoing proton momentum and polar angle, respectively. The central value as well as the square-root of the diagonal elements of the covariance matrix are given.

θ_{\min} (rad)	θ_{\max} (rad)	p_{\min} (GeV/ c)	p_{\max} (GeV/ c)	$d^2\sigma^p/(dpd\Omega)$ (barn/(sr GeV/ c))			
				3 GeV/c	5 GeV/c	8 GeV/c	12 GeV/c
0.050	0.100	0.50	1.00	0.12±0.05	0.13±0.03	0.10±0.02	0.09±0.02
			1.00	0.21±0.04	0.13±0.02	0.122±0.015	0.088±0.015
		1.50	2.00	0.31±0.05	0.16±0.02	0.16±0.02	0.090±0.015
			2.50	0.27±0.09	0.22±0.02	0.16±0.02	0.12±0.02
		2.50	3.00	±	0.33±0.03	0.20±0.02	0.15±0.01
			3.50	±	0.41±0.03	0.27±0.02	0.14±0.02
		3.50	4.00	±	0.40±0.03	0.30±0.02	0.18±0.02
			5.00	±	0.50±0.07	0.33±0.02	0.196±0.013
		5.00	6.50	±	±	0.24±0.01	0.191±0.010
			8.00	±	±	±	0.159±0.008
0.100	0.150	0.50	1.00	0.12±0.05	0.13±0.03	0.13±0.02	0.13±0.03
			1.00	0.22±0.04	0.12±0.02	0.11±0.02	0.14±0.02
		1.50	2.00	0.32±0.05	0.18±0.02	0.12±0.02	0.088±0.014
			2.50	0.30±0.05	0.19±0.02	0.14±0.02	0.080±0.013
		2.50	3.00	±	0.22±0.02	0.18±0.02	0.106±0.014
			3.00	±	0.22±0.02	0.177±0.015	0.099±0.012
		3.50	4.00	±	0.18±0.02	0.155±0.012	0.117±0.012
			5.00	±	0.19±0.03	0.137±0.011	0.112±0.010
		5.00	6.50	±	±	0.068±0.006	0.064±0.006
			8.00	±	±	±	0.038±0.004
0.150	0.200	0.50	1.00	0.08±0.04	0.13±0.03	0.07±0.02	0.10±0.02
			1.00	0.17±0.04	0.13±0.02	0.085±0.013	0.063±0.012
		1.50	2.00	0.15±0.03	0.14±0.02	0.088±0.012	0.076±0.014
			2.50	0.11±0.03	0.14±0.02	0.111±0.013	0.061±0.011
		2.50	3.00	±	0.122±0.014	0.098±0.011	0.063±0.010
			3.00	±	0.093±0.012	0.083±0.009	0.054±0.008
		3.50	4.00	±	0.079±0.011	0.067±0.007	0.042±0.006
			5.00	±	0.058±0.007	0.052±0.006	0.034±0.005
		5.00	6.50	±	±	0.015±0.003	0.015±0.003
			8.00	±	±	±	0.004±0.001
0.200	0.250	0.50	1.00	0.15±0.07	0.09±0.03	0.12±0.03	0.10±0.03
			1.00	0.14±0.04	0.10±0.02	0.10±0.02	0.07±0.02
		1.50	2.00	0.09±0.03	0.07±0.02	0.07±0.02	0.036±0.011
			2.50	0.08±0.03	0.059±0.013	0.09±0.02	0.054±0.015
		2.50	3.00	±	0.056±0.011	0.079±0.014	0.019±0.006
			3.00	±	0.031±0.007	0.060±0.009	0.020±0.005
		3.50	4.00	±	0.026±0.005	0.043±0.008	0.022±0.005
			5.00	±	0.026±0.005	0.027±0.005	0.014±0.004
		5.00	6.50	±	±	0.007±0.002	0.005±0.002
			8.00	±	±	±	0.002±0.001

TABLE VIII: HARP results for the double-differential p production cross-section in the laboratory system, $d^2\sigma^p/(dpd\Omega)$, for π^- -Al interactions at 3,5,8,12 GeV/c. Each row refers to a different ($p_{\min} \leq p < p_{\max}, \theta_{\min} \leq \theta < \theta_{\max}$) bin, where p and θ are the outgoing proton momentum and polar angle, respectively. The central value as well as the square-root of the diagonal elements of the covariance matrix are given.

θ_{\min} (rad)	θ_{\max} (rad)	p_{\min} (GeV/c)	p_{\max} (GeV/c)	$d^2\sigma^p/(dpd\Omega)$ (barn/(sr GeV/c))			
				3 GeV/c	5 GeV/c	8 GeV/c	12 GeV/c
0.050	0.100	0.50	1.00	0.16±0.03	0.15±0.04	0.15±0.03	0.12±0.03
			1.00	0.12±0.02	0.13±0.02	0.14±0.02	0.11±0.02
		1.50	2.00	0.075±0.013	0.12±0.02	0.14±0.02	0.08±0.02
			2.00	0.043±0.010	0.09±0.02	0.08±0.02	0.010±0.013
		2.50	3.00	±	0.047±0.011	0.104±0.013	0.08±0.02
			3.00	±	0.016±0.006	0.067±0.011	0.096±0.013
		3.50	4.00	±	0.033±0.009	0.067±0.009	0.086±0.011
			4.00	±	0.012±0.006	0.045±0.007	0.104±0.010
		5.00	6.50	±	±	0.010±0.003	0.042±0.006
			6.50	±	±	±	0.022±0.004
0.100	0.150	0.50	1.00	0.20±0.04	0.18±0.04	0.17±0.03	0.14±0.03
			1.00	0.14±0.02	0.19±0.03	0.15±0.02	0.15±0.02
		1.50	2.00	0.09±0.02	0.16±0.03	0.12±0.02	0.09±0.02
			2.00	0.047±0.010	0.10±0.02	0.11±0.02	0.06±0.02
		2.50	3.00	±	0.048±0.011	0.087±0.011	0.070±0.013
			3.00	±	0.021±0.007	0.056±0.011	0.097±0.015
		3.50	4.00	±	0.017±0.006	0.039±0.007	0.082±0.012
			4.00	±	0.008±0.004	0.025±0.005	0.053±0.008
		5.00	6.50	±	±	0.005±0.002	0.015±0.003
			6.50	±	±	±	0.004±0.001
0.150	0.200	0.50	1.00	0.16±0.04	0.09±0.03	0.16±0.03	0.15±0.03
			1.00	0.08±0.02	0.12±0.02	0.10±0.02	0.08±0.02
		1.50	2.00	0.061±0.013	0.10±0.02	0.12±0.02	0.09±0.02
			2.00	0.052±0.011	0.08±0.02	0.08±0.02	0.07±0.02
		2.50	3.00	±	0.027±0.008	0.068±0.012	0.054±0.011
			3.00	±	0.029±0.009	0.044±0.010	0.049±0.009
		3.50	4.00	±	0.002±0.002	0.026±0.006	0.045±0.008
			4.00	±	0.000±0.001	0.011±0.003	0.024±0.005
		5.00	6.50	±	±	0.001±0.001	0.004±0.001
			6.50	±	±	±	±
0.200	0.250	0.50	1.00	0.16±0.04	0.16±0.05	0.18±0.04	0.17±0.04
			1.00	0.14±0.03	0.18±0.04	0.21±0.04	0.15±0.03
		1.50	2.00	0.09±0.02	0.13±0.03	0.16±0.04	0.11±0.03
			2.00	0.030±0.012	0.09±0.02	0.13±0.03	0.08±0.03
		2.50	3.00	±	0.06±0.02	0.06±0.02	0.06±0.02
			3.00	±	0.019±0.009	0.024±0.008	0.036±0.009
		3.50	4.00	±	0.005±0.003	0.008±0.004	0.021±0.006
			4.00	±	0.001±0.002	0.003±0.002	0.012±0.005
		5.00	6.50	±	±	0.000±0.002	0.001±0.001
			6.50	±	±	±	0.000±0.001

TABLE IX: HARP results for the double-differential p production cross-section in the laboratory system, $d^2\sigma^p/(dpd\Omega)$, for π^+ -Al interactions at 3,5,8,12,12.9 GeV/c. Each row refers to a different ($p_{\min} \leq p < p_{\max}, \theta_{\min} \leq \theta < \theta_{\max}$) bin, where p and θ are the outgoing proton momentum and polar angle, respectively. The central value as well as the square-root of the diagonal elements of the covariance matrix are given.

θ_{\min} (rad)	θ_{\max} (rad)	p_{\min} (GeV/c)	p_{\max} (GeV/c)	$d^2\sigma^p/(dpd\Omega)$ (barn/(sr GeV/c))				
				3 GeV/c	5 GeV/c	8 GeV/c	12 GeV/c	12.9 GeV/c
0.050	0.100	0.50	1.00	0.16±0.06	0.17±0.04	0.14±0.04	0.17±0.19	0.18±0.05
			1.00	0.16±0.05	0.17±0.03	0.13±0.03	0.10±0.09	0.12±0.03
		1.50	2.00	±	0.13±0.03	0.11±0.03	0.05±0.08	0.14±0.03
			2.00	±	0.09±0.03	0.09±0.02	0.07±0.12	0.13±0.02
		2.50	3.00	±	±	0.07±0.02	0.07±0.08	0.12±0.02
			3.00	±	±	0.03±0.02	0.08±0.10	0.11±0.02
		3.50	4.00	±	±	±	0.02±0.08	0.10±0.02
			4.00	±	±	±	0.03±0.15	0.14±0.02
		5.00	6.50	±	±	±	0.005±0.092	0.075±0.010
			6.50	±	±	±	0.002±0.127	0.039±0.007
0.100	0.150	0.50	1.00	0.21±0.07	0.21±0.05	0.24±0.06	0.01±0.03	0.14±0.05
			1.00	0.15±0.04	0.13±0.03	0.13±0.03	0.11±0.08	0.14±0.03
		1.50	2.00	0.07±0.05	0.13±0.03	0.10±0.03	0.07±0.08	0.11±0.03
			2.00	±	0.05±0.07	0.08±0.02	0.06±0.06	0.09±0.02
		2.50	3.00	±	±	0.09±0.02	0.07±0.07	0.08±0.02
			3.00	±	±	0.05±0.02	0.02±0.03	0.09±0.02
		3.50	4.00	±	±	0.019±0.009	0.039±0.045	0.075±0.013
			4.00	±	±	0.017±0.007	0.064±0.075	0.068±0.012
		5.00	6.50	±	±	0.011±0.006	0.011±0.026	0.030±0.006
			6.50	±	±	±	0.005±0.016	0.010±0.003
0.150	0.200	0.50	1.00	0.19±0.07	0.20±0.04	0.20±0.05	0.10±0.14	0.08±0.04
			1.00	0.18±0.04	0.12±0.02	0.12±0.03	0.16±0.11	0.12±0.03
		1.50	2.00	0.05±0.04	0.11±0.02	0.07±0.02	0.15±0.11	0.08±0.02
			2.00	±	0.08±0.02	0.06±0.02	0.06±0.07	0.07±0.02
		2.50	3.00	±	0.02±0.02	0.08±0.02	0.013±0.032	0.051±0.015
			3.00	±	0.001±0.006	0.035±0.012	0.051±0.076	0.049±0.014
		3.50	4.00	±	0.013±0.011	0.013±0.008	0.028±0.044	0.037±0.010
			4.00	±	0.012±0.013	0.009±0.008	0.011±0.024	0.018±0.006
		5.00	6.50	±	±	0.002±0.002	0.006±0.015	0.010±0.003
			6.50	±	±	±	±	0.002±0.001
0.200	0.250	0.50	1.00	0.13±0.07	0.17±0.06	0.17±0.05	0.10±0.17	0.17±0.06
			1.00	0.14±0.05	0.11±0.03	0.11±0.03	0.08±0.13	0.08±0.02
		1.50	2.00	0.06±0.03	0.06±0.02	0.10±0.03	0.02±0.09	0.06±0.03
			2.00	0.04±0.03	0.06±0.02	0.09±0.03	0.13±0.22	0.06±0.02
		2.50	3.00	±	0.042±0.014	0.06±0.02	0.01±0.02	0.04±0.02
			3.00	±	0.019±0.009	0.04±0.02	0.079±0.116	0.031±0.009
		3.50	4.00	±	0.012±0.006	0.026±0.009	0.004±0.016	0.019±0.008
			4.00	±	0.009±0.004	0.021±0.009	0.000±0.004	0.008±0.005
		5.00	6.50	±	±	0.008±0.008	0.001±0.013	0.002±0.002
			6.50	±	±	±	0.000±0.004	0.001±0.001

TABLE X: HARP results for the double-differential p production cross-section in the laboratory system, $d^2\sigma^p/(dpd\Omega)$, for p-Al interactions at 3,5,8,12,12.9 GeV/c. Each row refers to a different ($p_{\min} \leq p < p_{\max}, \theta_{\min} \leq \theta < \theta_{\max}$) bin, where p and θ are the outgoing proton momentum and polar angle, respectively. The central value as well as the square-root of the diagonal elements of the covariance matrix are given.

θ_{\min} (rad)	θ_{\max} (rad)	p_{\min} (GeV/c)	p_{\max} (GeV/c)	$d^2\sigma^p/(dpd\Omega)$ (barn/(sr GeV/c))				
				3 GeV/c	5 GeV/c	8 GeV/c	12 GeV/c	12.9 GeV/c
0.050	0.100	0.50	1.00	0.20±0.08	0.22±0.05	0.22±0.04	0.22±0.05	0.23±0.03
			1.00	0.32±0.07	0.27±0.03	0.24±0.03	0.23±0.04	0.21±0.02
		1.50	2.00	0.41±0.08	0.33±0.04	0.23±0.02	0.26±0.04	0.21±0.02
			2.00	0.39±0.12	0.34±0.04	0.26±0.03	0.17±0.03	0.22±0.02
		2.50	3.00	±	0.53±0.04	0.35±0.03	0.26±0.03	0.25±0.02
			3.00	±	0.53±0.05	0.37±0.02	0.28±0.03	0.26±0.02
		3.50	4.00	±	0.59±0.05	0.35±0.02	0.30±0.03	0.30±0.02
			4.00	±	0.62±0.08	0.41±0.02	0.34±0.03	0.34±0.02
		5.00	6.50	±	±	0.35±0.02	0.31±0.02	0.312±0.011
			6.50	±	±	±	0.29±0.02	0.272±0.010
0.100	0.150	0.50	1.00	0.28±0.09	0.26±0.05	0.23±0.04	0.24±0.05	0.24±0.03
			1.00	0.30±0.07	0.29±0.04	0.18±0.03	0.26±0.04	0.22±0.02
		1.50	2.00	0.53±0.09	0.27±0.03	0.24±0.03	0.22±0.03	0.21±0.02
			2.00	0.44±0.08	0.35±0.04	0.23±0.03	0.18±0.03	0.21±0.02
		2.50	3.00	±	0.33±0.03	0.29±0.03	0.20±0.03	0.20±0.02
			3.00	±	0.34±0.04	0.28±0.02	0.20±0.03	0.20±0.02
		3.50	4.00	±	0.32±0.03	0.22±0.02	0.17±0.02	0.189±0.015
			4.00	±	0.32±0.05	0.20±0.02	0.20±0.02	0.190±0.013
		5.00	6.50	±	±	0.116±0.009	0.117±0.012	0.121±0.009
			6.50	±	±	±	0.076±0.009	0.063±0.006
0.150	0.200	0.50	1.00	0.19±0.08	0.27±0.06	0.18±0.04	0.22±0.05	0.21±0.03
			1.00	0.27±0.06	0.21±0.03	0.17±0.02	0.18±0.03	0.18±0.02
		1.50	2.00	0.25±0.06	0.22±0.03	0.15±0.02	0.15±0.03	0.15±0.02
			2.00	0.24±0.06	0.23±0.03	0.16±0.02	0.15±0.03	0.139±0.015
		2.50	3.00	±	0.17±0.03	0.15±0.02	0.10±0.02	0.127±0.012
			3.00	±	0.12±0.02	0.14±0.02	0.14±0.02	0.109±0.010
		3.50	4.00	±	0.11±0.02	0.094±0.011	0.082±0.014	0.086±0.008
			4.00	±	0.11±0.02	0.074±0.009	0.052±0.009	0.065±0.006
		5.00	6.50	±	±	0.036±0.005	0.022±0.004	0.027±0.003
			6.50	±	±	±	0.010±0.003	0.011±0.002
0.200	0.250	0.50	1.00	0.31±0.13	0.26±0.06	0.28±0.05	0.17±0.05	0.21±0.03
			1.00	0.12±0.05	0.18±0.04	0.20±0.04	0.12±0.04	0.16±0.02
		1.50	2.00	0.15±0.05	0.14±0.03	0.16±0.03	0.11±0.03	0.10±0.02
			2.00	0.10±0.04	0.12±0.03	0.14±0.03	0.08±0.03	0.09±0.02
		2.50	3.00	±	0.11±0.02	0.12±0.02	0.06±0.02	0.056±0.010
			3.00	±	0.08±0.02	0.064±0.011	0.042±0.012	0.039±0.006
		3.50	4.00	±	0.050±0.011	0.049±0.009	0.032±0.010	0.034±0.005
			4.00	±	0.031±0.008	0.045±0.008	0.023±0.009	0.030±0.005
		5.00	6.50	±	±	0.028±0.007	0.006±0.004	0.013±0.002
			6.50	±	±	±	0.007±0.004	0.007±0.001

TABLE XI: HARP results for the double-differential p production cross-section in the laboratory system, $d^2\sigma^p/(dpd\Omega)$, for π^- -Cu interactions at 3,5,8,12 GeV/c. Each row refers to a different ($p_{\min} \leq p < p_{\max}, \theta_{\min} \leq \theta < \theta_{\max}$) bin, where p and θ are the outgoing proton momentum and polar angle, respectively. The central value as well as the square-root of the diagonal elements of the covariance matrix are given.

θ_{\min} (rad)	θ_{\max} (rad)	p_{\min} (GeV/c)	p_{\max} (GeV/c)	$d^2\sigma^p/(dpd\Omega)$ (barn/(sr GeV/c))			
				3 GeV/c	5 GeV/c	8 GeV/c	12 GeV/c
0.050	0.100	0.50	1.00	0.31±0.05	0.35±0.05	0.42±0.06	0.33±0.07
			1.00	0.18±0.03	0.29±0.03	0.32±0.04	0.31±0.05
		1.50	2.00	0.13±0.02	0.21±0.03	0.31±0.04	0.26±0.05
			2.50	0.074±0.013	0.14±0.02	0.20±0.03	0.09±0.03
		2.50	3.00	±	0.075±0.013	0.20±0.02	0.17±0.03
			3.50	±	0.033±0.008	0.13±0.02	0.22±0.03
		3.50	4.00	±	0.021±0.006	0.13±0.02	0.17±0.03
			4.00	5.00	±	0.016±0.005	0.062±0.011
		5.00	6.50	±	±	0.018±0.005	0.071±0.010
			6.50	8.00	±	±	±
0.100	0.150	0.50	1.00	0.34±0.05	0.45±0.07	0.49±0.08	0.45±0.09
			1.00	0.24±0.03	0.35±0.04	0.33±0.04	0.41±0.06
		1.50	2.00	0.12±0.02	0.25±0.03	0.28±0.04	0.21±0.04
			2.50	0.080±0.013	0.17±0.02	0.20±0.03	0.12±0.03
		2.50	3.00	±	0.068±0.012	0.19±0.02	0.12±0.03
			3.00	3.50	±	0.050±0.009	0.10±0.02
		3.50	4.00	±	0.016±0.007	0.081±0.013	0.12±0.02
			4.00	5.00	±	0.011±0.004	0.046±0.009
		5.00	6.50	±	±	0.010±0.003	0.026±0.006
			6.50	8.00	±	±	±
0.150	0.200	0.50	1.00	0.30±0.05	0.38±0.06	0.40±0.07	0.36±0.08
			1.00	0.17±0.02	0.20±0.03	0.29±0.03	0.25±0.04
		1.50	2.00	0.08±0.02	0.16±0.02	0.23±0.03	0.19±0.04
			2.50	0.071±0.013	0.13±0.02	0.16±0.03	0.17±0.04
		2.50	3.00	±	0.063±0.011	0.11±0.02	0.12±0.02
			3.00	3.50	±	0.033±0.008	0.10±0.02
		3.50	4.00	±	0.009±0.004	0.052±0.011	0.08±0.02
			4.00	5.00	±	0.003±0.002	0.020±0.005
		5.00	6.50	±	±	0.000±0.001	0.009±0.003
			6.50	8.00	±	±	±
0.200	0.250	0.50	1.00	0.34±0.07	0.32±0.07	0.48±0.09	0.38±0.09
			1.00	0.26±0.04	0.33±0.05	0.48±0.08	0.45±0.09
		1.50	2.00	0.16±0.03	0.32±0.05	0.27±0.06	0.29±0.07
			2.50	0.07±0.02	0.19±0.03	0.31±0.06	0.31±0.08
		2.50	3.00	±	0.06±0.02	0.16±0.03	0.19±0.04
			3.00	3.50	±	0.024±0.008	0.047±0.013
		3.50	4.00	±	0.006±0.003	0.030±0.009	0.039±0.012
			4.00	5.00	±	0.003±0.002	0.016±0.005
		5.00	6.50	±	±	0.001±0.003	0.004±0.003
			6.50	8.00	±	±	±

TABLE XII: HARP results for the double-differential p production cross-section in the laboratory system, $d^2\sigma^p/(dpd\Omega)$, for π^+ -Cu interactions at 3,5,8,12 GeV/c. Each row refers to a different ($p_{\min} \leq p < p_{\max}, \theta_{\min} \leq \theta < \theta_{\max}$) bin, where p and θ are the outgoing proton momentum and polar angle, respectively. The central value as well as the square-root of the diagonal elements of the covariance matrix are given.

θ_{\min} (rad)	θ_{\max} (rad)	p_{\min} (GeV/c)	p_{\max} (GeV/c)	$d^2\sigma^p/(dpd\Omega)$ (barn/(sr GeV/c))			
				3 GeV/c	5 GeV/c	8 GeV/c	12 GeV/c
0.050	0.100	0.50	1.00	0.25±0.12	0.39±0.08	0.43±0.08	0.17±0.16
			1.00	0.28±0.10	0.36±0.05	0.32±0.06	0.48±0.21
		1.50	2.00	±	0.25±0.05	0.30±0.05	0.30±0.41
			2.00	±	0.05±0.05	0.16±0.04	0.19±0.32
		2.50	3.00	±	±	0.13±0.04	0.12±0.16
			3.00	±	±	0.09±0.04	0.07±0.07
		3.50	4.00	±	±	0.03±0.04	0.16±0.13
			4.00	±	±	±	0.10±0.12
		5.00	6.50	±	±	±	0.02±0.06
			6.50	±	±	±	0.01±0.07
0.100	0.150	0.50	1.00	0.30±0.13	0.47±0.09	0.53±0.11	0.69±0.36
			1.00	0.27±0.09	0.30±0.05	0.41±0.06	0.44±0.20
		1.50	2.00	0.07±0.08	0.26±0.05	0.24±0.05	0.32±0.17
			2.00	±	0.16±0.09	0.14±0.04	0.20±0.13
		2.50	3.00	±	±	0.13±0.03	0.15±0.11
			3.00	±	±	0.12±0.03	0.04±0.05
		3.50	4.00	±	±	0.04±0.02	0.11±0.09
			4.00	±	±	0.04±0.01	0.11±0.07
		5.00	6.50	±	±	0.02±0.02	0.04±0.04
			6.50	±	±	±	0.02±0.03
0.150	0.200	0.50	1.00	0.27±0.12	0.53±0.10	0.46±0.10	0.21±0.20
			1.00	0.27±0.08	0.23±0.04	0.30±0.05	0.34±0.18
		1.50	2.00	0.05±0.08	0.19±0.04	0.20±0.04	0.29±0.17
			2.00	±	0.07±0.03	0.15±0.04	0.23±0.14
		2.50	3.00	±	0.03±0.02	0.12±0.03	0.15±0.11
			3.00	±	0.01±0.02	0.10±0.03	0.08±0.09
		3.50	4.00	±	0.02±0.02	0.05±0.02	0.11±0.11
			4.00	±	0.01±0.02	0.02±0.01	0.02±0.04
		5.00	6.50	±	±	0.003±0.003	0.001±0.003
			6.50	±	±	±	0.006±0.025
0.200	0.250	0.50	1.00	0.32±0.17	0.33±0.10	0.39±0.10	0.05±0.12
			1.00	0.17±0.09	0.30±0.06	0.44±0.09	0.09±0.17
		1.50	2.00	0.08±0.05	0.12±0.04	0.16±0.05	0.04±0.14
			2.00	0.07±0.07	0.10±0.04	0.14±0.05	0.26±0.31
		2.50	3.00	±	0.06±0.02	0.09±0.03	0.09±0.22
			3.00	±	0.04±0.02	0.04±0.03	0.01±0.11
		3.50	4.00	±	0.03±0.01	0.02±0.02	±
			4.00	±	0.02±0.01	0.024±0.035	±
		5.00	6.50	±	±	0.009±0.012	±
			6.50	±	±	±	±

TABLE XIII: HARP results for the double-differential p production cross-section in the laboratory system, $d^2\sigma^p/(dpd\Omega)$, for p -Cu interactions at 3,5,8,12 GeV/ c . Each row refers to a different ($p_{\min} \leq p < p_{\max}, \theta_{\min} \leq \theta < \theta_{\max}$) bin, where p and θ are the outgoing proton momentum and polar angle, respectively. The central value as well as the square-root of the diagonal elements of the covariance matrix are given.

θ_{\min} (rad)	θ_{\max} (rad)	p_{\min} (GeV/ c)	p_{\max} (GeV/ c)	$d^2\sigma^p/(dpd\Omega)$ (barn/(sr GeV/ c))			
				3 GeV/c	5 GeV/c	8 GeV/c	12 GeV/c
0.050	0.100	0.50	1.00	0.48±0.19	0.45±0.09	0.53±0.08	0.51±0.09
			1.00	0.36±0.11	0.49±0.06	0.52±0.05	0.54±0.07
		1.50	2.00	0.40±0.11	0.54±0.07	0.54±0.05	0.46±0.06
			2.00	0.46±0.15	0.57±0.06	0.50±0.04	0.44±0.05
		2.50	3.00	±	0.76±0.08	0.55±0.05	0.57±0.05
			3.00	±	0.87±0.07	0.64±0.04	0.49±0.05
		3.50	4.00	±	0.77±0.07	0.66±0.05	0.52±0.05
			4.00	±	0.86±0.12	0.80±0.04	0.62±0.04
		5.00	6.50	±	±	0.54±0.03	0.51±0.03
			6.50	8.00	±	±	±
0.100	0.150	0.50	1.00	0.40±0.17	0.54±0.10	0.67±0.09	0.69±0.12
			1.00	0.59±0.15	0.49±0.07	0.48±0.05	0.48±0.07
		1.50	2.00	0.62±0.15	0.45±0.06	0.47±0.05	0.43±0.06
			2.00	0.52±0.12	0.50±0.07	0.41±0.04	0.44±0.06
		2.50	3.00	±	0.52±0.06	0.43±0.05	0.39±0.05
			3.00	±	0.50±0.06	0.49±0.04	0.35±0.04
		3.50	4.00	±	0.45±0.05	0.42±0.03	0.40±0.04
			4.00	±	0.50±0.06	0.34±0.03	0.35±0.03
		5.00	6.50	±	±	0.19±0.02	0.20±0.02
			6.50	8.00	±	±	±
0.150	0.200	0.50	1.00	0.37±0.16	0.54±0.11	0.61±0.10	0.57±0.11
			1.00	0.51±0.13	0.40±0.06	0.40±0.05	0.35±0.05
		1.50	2.00	0.45±0.13	0.43±0.05	0.32±0.04	0.29±0.05
			2.00	0.36±0.11	0.42±0.06	0.38±0.04	0.29±0.05
		2.50	3.00	±	0.23±0.04	0.28±0.03	0.17±0.03
			3.00	±	0.16±0.03	0.21±0.03	0.22±0.03
		3.50	4.00	±	0.17±0.03	0.16±0.02	0.16±0.02
			4.00	±	0.16±0.02	0.14±0.02	0.12±0.02
		5.00	6.50	±	±	0.051±0.008	0.034±0.007
			6.50	8.00	±	±	±
0.200	0.250	0.50	1.00	0.65±0.29	0.44±0.11	0.59±0.10	0.62±0.13
			1.00	0.23±0.12	0.43±0.08	0.40±0.07	0.36±0.08
		1.50	2.00	0.21±0.09	0.29±0.06	0.32±0.06	0.20±0.06
			2.00	0.27±0.11	0.18±0.04	0.26±0.05	0.18±0.05
		2.50	3.00	±	0.19±0.04	0.18±0.03	0.12±0.04
			3.00	±	0.08±0.02	0.13±0.02	0.09±0.02
		3.50	4.00	±	0.07±0.02	0.067±0.014	0.05±0.02
			4.00	±	0.06±0.02	0.063±0.013	0.043±0.014
		5.00	6.50	±	±	0.024±0.006	0.027±0.010
			6.50	8.00	±	±	±

TABLE XIV: HARP results for the double-differential p production cross-section in the laboratory system, $d^2\sigma^p/(dpd\Omega)$, for π^- -Sn interactions at 3,5,8,12 GeV/c. Each row refers to a different ($p_{\min} \leq p < p_{\max}, \theta_{\min} \leq \theta < \theta_{\max}$) bin, where p and θ are the outgoing proton momentum and polar angle, respectively. The central value as well as the square-root of the diagonal elements of the covariance matrix are given.

θ_{\min} (rad)	θ_{\max} (rad)	p_{\min} (GeV/c)	p_{\max} (GeV/c)	$d^2\sigma^p/(dpd\Omega)$ (barn/(sr GeV/c))			
				3 GeV/c	5 GeV/c	8 GeV/c	12 GeV/c
0.050	0.100	0.50	1.00	0.52±0.09	0.67±0.10	0.79±0.11	0.75±0.11
			1.00	0.26±0.05	0.45±0.05	0.51±0.07	0.55±0.06
		1.50	2.00	0.15±0.03	0.30±0.04	0.47±0.06	0.41±0.08
			2.00	0.05±0.02	0.19±0.03	0.24±0.05	0.11±0.34
		2.50	3.00	±	0.09±0.02	0.26±0.03	0.27±0.07
			3.00	±	0.043±0.013	0.12±0.03	0.33±0.07
		3.50	4.00	±	0.029±0.009	0.14±0.02	0.25±0.04
			4.00	±	0.014±0.007	0.07±0.02	0.22±0.03
		5.00	6.50	±	±	0.019±0.007	0.121±0.015
			6.50	8.00	±	±	±
0.100	0.150	0.50	1.00	0.53±0.09	0.62±0.10	0.82±0.13	0.81±0.13
			1.00	0.33±0.06	0.55±0.07	0.61±0.08	0.72±0.08
		1.50	2.00	0.16±0.03	0.32±0.04	0.38±0.06	0.42±0.07
			2.00	0.06±0.02	0.21±0.03	0.32±0.04	0.22±0.07
		2.50	3.00	±	0.10±0.02	0.21±0.03	0.30±0.04
			3.00	±	0.050±0.012	0.15±0.03	0.22±0.04
		3.50	4.00	±	0.019±0.007	0.12±0.02	0.17±0.02
			4.00	±	0.017±0.007	0.041±0.011	0.14±0.02
		5.00	6.50	±	±	0.009±0.003	0.052±0.010
			6.50	8.00	±	±	±
0.150	0.200	0.50	1.00	0.51±0.10	0.82±0.13	0.66±0.12	0.58±0.11
			1.00	0.19±0.04	0.37±0.05	0.44±0.06	0.58±0.07
		1.50	2.00	0.09±0.03	0.28±0.04	0.37±0.05	0.24±0.05
			2.00	0.04±0.02	0.15±0.03	0.21±0.05	0.22±0.10
		2.50	3.00	±	0.07±0.02	0.17±0.03	0.27±0.07
			3.00	±	0.024±0.008	0.13±0.03	0.15±0.03
		3.50	4.00	±	0.007±0.004	0.08±0.02	0.09±0.02
			4.00	±	0.003±0.003	0.020±0.006	0.071±0.014
		5.00	6.50	±	±	0.001±0.001	0.011±0.004
			6.50	8.00	±	±	±
0.200	0.250	0.50	1.00	0.57±0.13	0.69±0.13	0.83±0.16	0.73±0.14
			1.00	0.29±0.07	0.60±0.09	0.86±0.14	0.70±0.12
		1.50	2.00	0.14±0.04	0.35±0.06	0.48±0.10	0.53±0.11
			2.00	0.07±0.03	0.18±0.04	0.43±0.08	0.37±0.10
		2.50	3.00	±	0.11±0.03	0.17±0.05	0.27±0.06
			3.00	±	0.025±0.012	0.04±0.02	0.12±0.04
		3.50	4.00	±	0.005±0.003	0.016±0.009	0.06±0.02
			4.00	±	0.003±0.002	0.007±0.004	0.04±0.02
		5.00	6.50	±	±	0.001±0.006	0.008±0.004
			6.50	8.00	±	±	±

TABLE XV: HARP results for the double-differential p production cross-section in the laboratory system, $d^2\sigma^p/(dpd\Omega)$, for π^+ -Sn interactions at 3,5,8,12 GeV/c. Each row refers to a different ($p_{\min} \leq p < p_{\max}, \theta_{\min} \leq \theta < \theta_{\max}$) bin, where p and θ are the outgoing proton momentum and polar angle, respectively. The central value as well as the square-root of the diagonal elements of the covariance matrix are given.

θ_{\min} (rad)	θ_{\max} (rad)	p_{\min} (GeV/c)	p_{\max} (GeV/c)	$d^2\sigma^p/(dpd\Omega)$ (barn/(sr GeV/c))			
				3 GeV/c	5 GeV/c	8 GeV/c	12 GeV/c
0.050	0.100	0.50	1.00	0.49±0.16	0.70±0.13	0.66±0.12	0.75±0.27
			1.00	0.23±0.10	0.54±0.07	0.62±0.09	0.54±0.17
		1.50	2.00	±	0.37±0.12	0.50±0.08	0.45±0.60
			2.00	±	0.01±0.03	0.36±0.07	0.21±0.32
		2.50	3.00	±	±	0.15±0.06	0.26±0.25
			3.00	±	±	0.05±0.11	0.21±0.11
		3.50	4.00	±	±	0.01±0.33	0.21±0.10
			4.00	±	±	±	0.12±0.08
		5.00	6.50	±	±	±	±
			6.50	8.00	±	±	±
0.100	0.150	0.50	1.00	0.55±0.17	0.84±0.15	1.03±0.19	0.88±0.30
			1.00	0.43±0.12	0.51±0.08	0.58±0.09	0.76±0.21
		1.50	2.00	0.14±0.12	0.41±0.08	0.48±0.08	0.36±0.14
			2.00	±	0.10±0.06	0.22±0.05	0.33±0.14
		2.50	3.00	±	±	0.20±0.04	0.19±0.10
			3.00	±	±	0.21±0.06	0.08±0.06
		3.50	4.00	±	±	0.08±0.04	0.15±0.09
			4.00	±	±	0.08±0.04	0.14±0.07
		5.00	6.50	±	±	0.01±0.02	0.05±0.06
			6.50	8.00	±	±	±
0.150	0.200	0.50	1.00	0.64±0.19	0.96±0.16	0.67±0.14	0.74±0.30
			1.00	0.29±0.08	0.42±0.06	0.48±0.08	0.63±0.19
		1.50	2.00	±	0.30±0.05	0.38±0.07	0.43±0.16
			2.00	±	0.10±0.05	0.23±0.05	0.25±0.12
		2.50	3.00	±	0.00±0.00	0.13±0.03	0.04±0.04
			3.00	±	±	0.08±0.03	0.09±0.06
		3.50	4.00	±	±	0.06±0.02	0.17±0.09
			4.00	±	±	0.041±0.013	0.05±0.04
		5.00	6.50	±	±	0.005±0.003	0.002±0.005
			6.50	8.00	±	±	±
0.200	0.250	0.50	1.00	0.34±0.17	0.64±0.18	0.95±0.21	0.50±0.27
			1.00	0.19±0.09	0.46±0.09	0.68±0.14	0.79±0.33
		1.50	2.00	0.09±0.06	0.17±0.06	0.39±0.10	0.14±0.15
			2.00	0.08±0.07	0.07±0.04	0.31±0.09	0.13±0.13
		2.50	3.00	±	0.07±0.03	0.12±0.04	0.11±0.11
			3.00	±	0.04±0.02	0.08±0.03	0.07±0.08
		3.50	4.00	±	0.02±0.02	0.06±0.02	0.09±0.09
			4.00	±	0.01±0.01	0.07±0.03	0.05±0.07
		5.00	6.50	±	±	0.02±0.01	0.01±0.02
			6.50	8.00	±	±	±

TABLE XVI: HARP results for the double-differential p production cross-section in the laboratory system, $d^2\sigma^p/(dpd\Omega)$, for p-C interactions at 3,5,8,12 GeV/c. Each row refers to a different ($p_{\min} \leq p < p_{\max}, \theta_{\min} \leq \theta < \theta_{\max}$) bin, where p and θ are the outgoing proton momentum and polar angle, respectively. The central value as well as the square-root of the diagonal elements of the covariance matrix are given.

θ_{\min} (rad)	θ_{\max} (rad)	p_{\min} (GeV/c)	p_{\max} (GeV/c)	$d^2\sigma^p/(dpd\Omega)$ (barn/(sr GeV/c))			
				3 GeV/c	5 GeV/c	8 GeV/c	12 GeV/c
0.050	0.100	0.50	1.00	0.46±0.16	0.73±0.13	0.94±0.12	1.08±0.13
			1.00	0.45±0.11	0.73±0.08	0.88±0.08	0.85±0.07
		1.50	2.00	0.35±0.09	0.66±0.08	0.76±0.07	0.73±0.07
			2.00	0.24±0.08	0.59±0.08	0.72±0.06	0.59±0.05
		2.50	3.00	±	0.99±0.10	0.74±0.06	0.72±0.06
			3.00	±	1.05±0.09	0.89±0.06	0.68±0.05
		3.50	4.00	±	1.08±0.11	0.86±0.06	0.71±0.06
			4.00	±	1.12±0.13	1.02±0.05	0.81±0.05
		5.00	6.50	±	±	0.68±0.04	0.68±0.03
			6.50	±	±	±	0.56±0.03
0.100	0.150	0.50	1.00	0.57±0.18	0.94±0.15	1.19±0.16	1.28±0.17
			1.00	0.70±0.15	0.68±0.10	0.89±0.09	0.97±0.09
		1.50	2.00	0.57±0.14	0.67±0.08	0.68±0.07	0.82±0.08
			2.00	0.64±0.13	0.62±0.09	0.63±0.07	0.61±0.06
		2.50	3.00	±	0.68±0.08	0.68±0.06	0.53±0.05
			3.00	±	0.65±0.07	0.65±0.06	0.48±0.05
		3.50	4.00	±	0.52±0.06	0.54±0.04	0.55±0.05
			4.00	±	0.54±0.08	0.49±0.04	0.51±0.04
		5.00	6.50	±	±	0.20±0.02	0.25±0.02
			6.50	±	±	±	0.140±0.015
0.150	0.200	0.50	1.00	0.57±0.19	1.15±0.18	1.08±0.15	0.96±0.14
			1.00	0.43±0.11	0.52±0.07	0.61±0.07	0.63±0.07
		1.50	2.00	0.34±0.11	0.50±0.07	0.54±0.06	0.55±0.06
			2.00	0.40±0.12	0.39±0.06	0.45±0.05	0.45±0.05
		2.50	3.00	±	0.36±0.06	0.45±0.05	0.33±0.04
			3.00	±	0.24±0.04	0.33±0.03	0.33±0.04
		3.50	4.00	±	0.16±0.03	0.23±0.03	0.25±0.03
			4.00	±	0.18±0.03	0.18±0.02	0.17±0.02
		5.00	6.50	±	±	0.065±0.010	0.068±0.009
			6.50	±	±	±	0.023±0.005
0.200	0.250	0.50	1.00	0.63±0.26	0.72±0.16	1.18±0.18	0.97±0.16
			1.00	0.17±0.09	0.61±0.11	0.77±0.11	0.74±0.11
		1.50	2.00	0.15±0.06	0.32±0.07	0.47±0.08	0.40±0.07
			2.00	0.21±0.08	0.23±0.06	0.45±0.08	0.39±0.07
		2.50	3.00	±	0.23±0.05	0.29±0.05	0.23±0.04
			3.00	±	0.08±0.02	0.23±0.03	0.18±0.03
		3.50	4.00	±	0.08±0.02	0.15±0.03	0.11±0.02
			4.00	±	0.06±0.02	0.12±0.02	0.08±0.02
		5.00	6.50	±	±	0.044±0.011	0.037±0.010
			6.50	±	±	±	0.018±0.005

TABLE XVII: HARP results for the double-differential p production cross-section in the laboratory system, $d^2\sigma^p/(dpd\Omega)$, for π^- -Ta interactions at 3,5,8,12 GeV/c. Each row refers to a different ($p_{\min} \leq p < p_{\max}, \theta_{\min} \leq \theta < \theta_{\max}$) bin, where p and θ are the outgoing proton momentum and polar angle, respectively. The central value as well as the square-root of the diagonal elements of the covariance matrix are given.

θ_{\min} (rad)	θ_{\max} (rad)	p_{\min} (GeV/c)	p_{\max} (GeV/c)	$d^2\sigma^p/(dpd\Omega)$ (barn/(sr GeV/c))			
				3 GeV/c	5 GeV/c	8 GeV/c	12 GeV/c
0.050	0.100	0.50	1.00	0.64±0.15	0.81±0.12	1.17±0.16	0.91±0.14
			1.00	0.30±0.08	0.54±0.07	0.84±0.10	0.85±0.10
		1.50	2.00	0.08±0.03	0.40±0.06	0.61±0.08	0.50±0.08
			2.50	0.01±0.01	0.26±0.04	0.32±0.06	0.25±0.07
		2.50	3.00	±	0.09±0.02	0.29±0.04	0.40±0.06
			3.50	±	0.04±0.02	0.19±0.04	0.41±0.05
		3.50	4.00	±	0.02±0.01	0.16±0.03	0.32±0.04
			4.00	5.00	±	0.01±0.01	0.11±0.02
		5.00	6.50	±	±	0.029±0.010	0.15±0.02
			6.50	8.00	±	±	±
0.100	0.150	0.50	1.00	0.72±0.17	1.16±0.17	1.20±0.18	1.42±0.21
			1.00	0.53±0.12	0.71±0.09	0.71±0.09	1.06±0.12
		1.50	2.00	0.06±0.03	0.43±0.06	0.48±0.08	0.53±0.08
			2.00	2.50	0.03±0.02	0.23±0.04	0.40±0.06
		2.50	3.00	±	0.09±0.02	0.24±0.03	0.29±0.05
			3.00	3.50	±	0.04±0.01	0.16±0.04
		3.50	4.00	±	0.02±0.01	0.12±0.03	0.23±0.03
			4.00	5.00	±	0.004±0.003	0.11±0.02
		5.00	6.50	±	±	0.01±0.01	0.08±0.01
			6.50	8.00	±	±	±
0.150	0.200	0.50	1.00	0.88±0.21	0.92±0.15	0.93±0.15	1.06±0.17
			1.00	0.19±0.06	0.45±0.07	0.51±0.07	0.54±0.07
		1.50	2.00	0.06±0.03	0.31±0.05	0.40±0.05	0.56±0.08
			2.00	2.50	0.07±0.03	0.21±0.04	0.22±0.05
		2.50	3.00	±	0.10±0.02	0.22±0.04	0.33±0.05
			3.00	3.50	±	0.03±0.01	0.14±0.03
		3.50	4.00	±	0.02±0.01	0.08±0.02	0.14±0.02
			4.00	5.00	±	0.006±0.004	0.02±0.01
		5.00	6.50	±	±	±	0.02±0.01
			6.50	8.00	±	±	±
0.200	0.250	0.50	1.00	0.70±0.22	1.10±0.20	1.42±0.25	1.23±0.22
			1.00	0.53±0.16	0.67±0.12	1.06±0.17	1.02±0.17
		1.50	2.00	0.13±0.07	0.52±0.09	0.69±0.14	0.61±0.13
			2.00	2.50	0.05±0.05	0.22±0.05	0.36±0.08
		2.50	3.00	±	0.07±0.03	0.26±0.07	0.36±0.08
			3.00	3.50	±	0.03±0.02	0.04±0.02
		3.50	4.00	±	0.01±0.01	0.03±0.01	0.09±0.02
			4.00	5.00	±	0.004±0.003	0.03±0.01
		5.00	6.50	±	±	0.004±0.006	0.01±0.02
			6.50	8.00	±	±	±

TABLE XVIII: HARP results for the double-differential p production cross-section in the laboratory system, $d^2\sigma^p/(dpd\Omega)$, for π^+ -Ta interactions at 3,5,8,12 GeV/c. Each row refers to a different ($p_{\min} \leq p < p_{\max}, \theta_{\min} \leq \theta < \theta_{\max}$) bin, where p and θ are the outgoing proton momentum and polar angle, respectively. The central value as well as the square-root of the diagonal elements of the covariance matrix are given.

θ_{\min} (rad)	θ_{\max} (rad)	p_{\min} (GeV/c)	p_{\max} (GeV/c)	$d^2\sigma^p/(dpd\Omega)$ (barn/(sr GeV/c))			
				3 GeV/c	5 GeV/c	8 GeV/c	12 GeV/c
0.050	0.100	0.50	1.00	0.46±0.17	0.98±0.19	1.28±0.21	1.61±0.63
			1.00	0.21±0.11	0.66±0.11	0.91±0.14	0.63±0.32
		1.50	2.00	±	0.37±0.14	0.71±0.11	0.67±0.90
			2.50	±	±	0.50±0.10	0.23±0.54
		2.50	3.00	±	±	0.15±0.07	0.51±0.54
			3.50	±	±	0.06±0.08	0.62±1.28
		3.50	4.00	±	±	0.07±0.04	0.34±0.85
			4.00	5.00	±	±	±
		5.00	6.50	±	±	±	±
			6.50	8.00	±	±	±
0.100	0.150	0.50	1.00	0.82±0.25	1.11±0.21	1.52±0.28	1.47±0.62
			1.00	0.39±0.13	0.62±0.12	0.83±0.13	0.55±0.31
		1.50	2.00	0.03±0.10	0.41±0.11	0.52±0.10	0.60±0.31
			2.50	±	0.04±0.07	0.31±0.08	0.43±0.26
		2.50	3.00	±	±	0.27±0.07	0.35±0.23
			3.00	3.50	±	±	0.13±0.05
		3.50	4.00	±	±	0.13±0.05	0.04±0.07
			4.00	5.00	±	±	0.05±0.03
		5.00	6.50	±	±	0.02±0.14	0.05±0.07
			6.50	8.00	±	±	±
0.150	0.200	0.50	1.00	0.37±0.15	1.03±0.20	1.16±0.23	1.39±0.67
			1.00	0.35±0.11	0.46±0.09	0.75±0.12	0.66±0.33
		1.50	2.00	0.04±0.13	0.38±0.08	0.36±0.09	0.29±0.22
			2.50	±	0.20±0.11	0.23±0.07	0.22±0.20
		2.50	3.00	±	0.03±0.10	0.21±0.06	0.19±0.18
			3.00	3.50	±	0.01±0.04	0.12±0.05
		3.50	4.00	±	±	0.07±0.03	0.14±0.14
			4.00	5.00	±	±	0.02±0.01
		5.00	6.50	±	±	0.001±0.001	0.01±0.03
			6.50	8.00	±	±	±
0.200	0.250	0.50	1.00	0.67±0.29	0.93±0.27	1.25±0.29	1.19±0.71
			1.00	0.20±0.11	0.52±0.12	0.69±0.16	0.86±0.51
		1.50	2.00	0.09±0.09	0.19±0.08	0.45±0.13	0.66±0.53
			2.50	0.15±0.11	0.12±0.07	0.29±0.10	0.58±0.43
		2.50	3.00	±	0.09±0.04	0.14±0.05	0.14±0.16
			3.00	3.50	±	0.02±0.01	0.08±0.03
		3.50	4.00	±	0.04±0.04	0.04±0.02	0.10±0.16
			4.00	5.00	±	0.05±0.03	0.04±0.02
		5.00	6.50	±	±	0.00±0.01	0.06±0.16
			6.50	8.00	±	±	±

TABLE XIX: HARP results for the double-differential p production cross-section in the laboratory system, $d^2\sigma^p/(dpd\Omega)$, for p-Ta interactions at 3,5,8,12 GeV/c. Each row refers to a different ($p_{\min} \leq p < p_{\max}, \theta_{\min} \leq \theta < \theta_{\max}$) bin, where p and θ are the outgoing proton momentum and polar angle, respectively. The central value as well as the square-root of the diagonal elements of the covariance matrix are given.

θ_{\min} (rad)	θ_{\max} (rad)	p_{\min} (GeV/c)	p_{\max} (GeV/c)	$d^2\sigma^p/(dpd\Omega)$ (barn/(sr GeV/c))			
				3 GeV/c	5 GeV/c	8 GeV/c	12 GeV/c
0.050	0.100	0.50	1.00	0.52±0.18	1.12±0.20	1.57±0.20	1.76±0.24
			1.00	0.45±0.12	0.88±0.12	1.14±0.11	1.18±0.13
		1.50	2.00	0.18±0.06	0.61±0.11	1.02±0.10	1.16±0.13
			2.50	0.19±0.07	0.75±0.12	0.86±0.08	0.88±0.10
		2.50	3.00	±	0.90±0.11	0.98±0.08	0.90±0.09
			3.50	±	1.20±0.16	0.91±0.08	0.80±0.09
		3.50	4.00	±	1.14±0.15	1.08±0.09	0.83±0.08
			4.00	5.00	±	0.93±0.14	1.20±0.07
		5.00	6.50	±	±	0.73±0.05	0.87±0.05
			6.50	8.00	±	±	±
0.100	0.150	0.50	1.00	0.94±0.26	1.26±0.22	1.75±0.23	1.60±0.25
			1.00	0.79±0.18	0.82±0.14	1.08±0.12	1.30±0.15
		1.50	2.00	0.69±0.18	0.62±0.10	0.81±0.10	1.06±0.13
			2.50	0.55±0.12	0.50±0.10	0.74±0.08	0.80±0.10
		2.50	3.00	±	0.70±0.10	0.73±0.07	0.62±0.08
			3.00	3.50	±	0.73±0.11	0.79±0.07
		3.50	4.00	±	0.62±0.11	0.65±0.06	0.61±0.07
			4.00	5.00	±	0.53±0.09	0.58±0.05
		5.00	6.50	±	±	0.27±0.03	0.31±0.03
			6.50	8.00	±	±	±
0.150	0.200	0.50	1.00	0.79±0.23	1.38±0.25	1.42±0.21	1.70±0.28
			1.00	0.61±0.15	0.72±0.11	0.91±0.10	1.05±0.13
		1.50	2.00	0.40±0.13	0.65±0.10	0.71±0.08	0.69±0.10
			2.50	0.37±0.13	0.51±0.09	0.56±0.07	0.57±0.09
		2.50	3.00	±	0.41±0.08	0.53±0.06	0.62±0.08
			3.00	3.50	±	0.18±0.04	0.36±0.04
		3.50	4.00	±	0.18±0.04	0.34±0.04	0.29±0.04
			4.00	5.00	±	0.19±0.04	0.18±0.03
		5.00	6.50	±	±	0.058±0.013	0.08±0.02
			6.50	8.00	±	±	±
0.200	0.250	0.50	1.00	1.37±0.44	0.98±0.24	1.73±0.27	1.74±0.31
			1.00	0.36±0.14	0.52±0.12	0.92±0.15	0.96±0.18
		1.50	2.00	0.11±0.05	0.30±0.09	0.39±0.08	0.51±0.13
			2.50	0.22±0.08	0.20±0.07	0.40±0.08	0.41±0.11
		2.50	3.00	±	0.28±0.07	0.25±0.05	0.25±0.06
			3.00	3.50	±	0.10±0.03	0.21±0.04
		3.50	4.00	±	0.10±0.03	0.15±0.03	0.25±0.05
			4.00	5.00	±	0.12±0.03	0.11±0.03
		5.00	6.50	±	±	0.047±0.014	0.042±0.013
			6.50	8.00	±	±	±

TABLE XX: HARP results for the double-differential p production cross-section in the laboratory system, $d^2\sigma^p/(dpd\Omega)$, for π^- -Pb interactions at 3,5,8,12 GeV/c. Each row refers to a different ($p_{\min} \leq p < p_{\max}, \theta_{\min} \leq \theta < \theta_{\max}$) bin, where p and θ are the outgoing proton momentum and polar angle, respectively. The central value as well as the square-root of the diagonal elements of the covariance matrix are given.

θ_{\min} (rad)	θ_{\max} (rad)	p_{\min} (GeV/c)	p_{\max} (GeV/c)	$d^2\sigma^p/(dpd\Omega)$ (barn/(sr GeV/c))			
				3 GeV/c	5 GeV/c	8 GeV/c	12 GeV/c
0.050	0.100	0.50	1.00	0.67±0.16	1.10±0.14	1.22±0.16	1.24±0.16
			1.00	0.11±0.05	0.54±0.06	0.82±0.10	0.89±0.09
		1.50	2.00	0.10±0.04	0.45±0.05	0.73±0.09	0.59±0.09
			2.50	0.03±0.02	0.21±0.03	0.31±0.06	0.13±0.07
		2.50	3.00	±	0.12±0.02	0.30±0.04	0.35±0.07
			3.50	±	0.05±0.02	0.19±0.04	0.32±0.04
		3.50	4.00	±	0.03±0.01	0.24±0.04	0.34±0.04
			5.00	±	0.01±0.01	0.11±0.02	0.32±0.03
		5.00	6.50	±	±	0.03±0.01	0.15±0.02
			8.00	±	±	±	0.05±0.01
0.100	0.150	0.50	1.00	0.75±0.18	1.30±0.17	1.32±0.20	1.38±0.19
			1.50	0.34±0.10	0.74±0.08	0.96±0.11	1.06±0.11
		1.50	2.00	0.07±0.03	0.44±0.06	0.60±0.09	0.53±0.09
			2.50	0.06±0.03	0.21±0.03	0.36±0.06	0.24±0.06
		2.50	3.00	±	0.12±0.02	0.31±0.04	0.38±0.05
			3.50	±	0.06±0.02	0.17±0.04	0.31±0.04
		3.50	4.00	±	0.03±0.01	0.15±0.03	0.21±0.03
			5.00	±	0.02±0.01	0.08±0.02	0.17±0.02
		5.00	6.50	±	±	0.01±0.01	0.08±0.01
			8.00	±	±	±	0.015±0.004
0.150	0.200	0.50	1.00	0.44±0.14	1.19±0.17	1.37±0.20	1.33±0.19
			1.50	0.17±0.06	0.47±0.06	0.60±0.08	0.68±0.08
		1.50	2.00	0.03±0.02	0.35±0.05	0.51±0.07	0.55±0.08
			2.50	0.04±0.03	0.20±0.04	0.32±0.06	0.37±0.07
		2.50	3.00	±	0.063±0.015	0.21±0.04	0.30±0.04
			3.50	±	0.02±0.01	0.11±0.03	0.23±0.03
		3.50	4.00	±	0.02±0.01	0.11±0.03	0.17±0.02
			5.00	±	0.01±0.01	0.02±0.01	0.10±0.02
		5.00	6.50	±	±	±	0.02±0.01
			8.00	±	±	±	0.003±0.001
0.200	0.250	0.50	1.00	0.55±0.21	1.08±0.19	1.29±0.23	1.54±0.25
			1.50	0.51±0.17	0.82±0.12	1.18±0.19	1.10±0.16
		1.50	2.00	0.09±0.06	0.42±0.07	0.74±0.15	0.86±0.16
			2.50	0.01±0.01	0.34±0.06	0.64±0.13	0.61±0.12
		2.50	3.00	±	0.08±0.03	0.33±0.07	0.47±0.08
			3.50	±	0.03±0.02	0.09±0.04	0.18±0.04
		3.50	4.00	±	0.007±0.004	0.04±0.02	0.05±0.02
			5.00	±	0.003±0.002	0.02±0.01	0.04±0.01
		5.00	6.50	±	±	0.001±0.006	0.009±0.003
			8.00	±	±	±	0.003±0.002

TABLE XXI: HARP results for the double-differential p production cross-section in the laboratory system, $d^2\sigma^p/(dpd\Omega)$, for π^+ -Pb interactions at 3,5,8,12 GeV/c. Each row refers to a different ($p_{\min} \leq p < p_{\max}, \theta_{\min} \leq \theta < \theta_{\max}$) bin, where p and θ are the outgoing proton momentum and polar angle, respectively. The central value as well as the square-root of the diagonal elements of the covariance matrix are given.

θ_{\min} (rad)	θ_{\max} (rad)	p_{\min} (GeV/c)	p_{\max} (GeV/c)	$d^2\sigma^p/(dpd\Omega)$ (barn/(sr GeV/c))			
				3 GeV/c	5 GeV/c	8 GeV/c	12 GeV/c
0.050	0.100	0.50	1.00	0.70±0.23	0.93±0.21	1.47±0.23	1.47±0.90
			1.00	0.37±0.15	0.71±0.12	0.75±0.12	1.17±0.66
		1.50	2.00	±	0.31±0.11	0.68±0.12	0.34±0.52
			2.00	±	0.03±0.07	0.44±0.10	0.24±0.42
		2.50	3.00	±	±	0.21±0.09	0.02±0.11
			3.00	±	±	0.08±0.08	0.15±0.35
		3.50	4.00	±	±	±	0.08±0.19
			4.00	±	±	±	0.17±0.34
		5.00	6.50	±	±	±	1.89±0.30
			6.50	±	±	±	±
0.100	0.150	0.50	1.00	0.69±0.24	1.23±0.24	1.68±0.29	0.28±0.37
			1.00	0.30±0.13	0.47±0.11	0.70±0.12	1.15±0.66
		1.50	2.00	0.02±0.06	0.44±0.12	0.54±0.11	1.22±0.66
			2.00	±	0.13±0.09	0.22±0.09	0.45±0.39
		2.50	3.00	±	±	0.27±0.15	0.46±0.43
			3.00	±	±	0.16±0.17	0.07±0.19
		3.50	4.00	±	±	0.10±0.24	0.13±0.31
			4.00	±	±	0.04±0.11	0.11±0.45
		5.00	6.50	±	±	0.02±0.11	0.03±0.20
			6.50	±	±	±	0.00±0.10
0.150	0.200	0.50	1.00	0.61±0.21	1.19±0.23	1.18±0.24	0.23±0.47
			1.00	0.45±0.13	0.53±0.10	0.65±0.11	0.81±0.52
		1.50	2.00	0.00±0.00	0.34±0.08	0.44±0.10	0.51±0.47
			2.00	±	0.07±0.07	0.20±0.07	0.37±0.39
		2.50	3.00	±	0.01±0.06	0.18±0.05	0.20±0.37
			3.00	±	±	0.07±0.03	0.05±0.34
		3.50	4.00	±	0.03±0.07	0.05±0.03	0.00±0.12
			4.00	±	0.04±0.05	0.02±0.02	0.01±0.16
		5.00	6.50	±	±	0.00±0.00	0.01±0.08
			6.50	±	±	±	0.00±0.13
0.200	0.250	0.50	1.00	0.46±0.27	1.23±0.34	1.30±0.29	1.50±1.27
			1.00	0.08±0.07	0.61±0.14	0.61±0.15	1.41±0.96
		1.50	2.00	0.15±0.08	0.18±0.08	0.22±0.08	0.74±0.90
			2.00	0.09±0.11	0.13±0.08	0.30±0.11	0.66±1.00
		2.50	3.00	±	0.10±0.06	0.16±0.06	0.07±0.29
			3.00	±	0.06±0.05	0.08±0.03	0.18±0.52
		3.50	4.00	±	0.03±0.03	0.05±0.02	0.16±0.54
			4.00	±	0.03±0.02	0.03±0.02	±
		5.00	6.50	±	±	0.01±0.01	±
			6.50	±	±	±	±

TABLE XXII: HARP results for the double-differential p production cross-section in the laboratory system, $d^2\sigma^p/(dpd\Omega)$, for p-Pb interactions at 3,5,8,12 GeV/c. Each row refers to a different ($p_{\min} \leq p < p_{\max}, \theta_{\min} \leq \theta < \theta_{\max}$) bin, where p and θ are the outgoing proton momentum and polar angle, respectively. The central value as well as the square-root of the diagonal elements of the covariance matrix are given.

θ_{\min} (rad)	θ_{\max} (rad)	p_{\min} (GeV/c)	p_{\max} (GeV/c)	$d^2\sigma^p/(dpd\Omega)$ (barn/(sr GeV/c))			
				3 GeV/c	5 GeV/c	8 GeV/c	12 GeV/c
0.050	0.100	0.50	1.00	0.63±0.22	1.17±0.23	1.62±0.20	1.92±0.31
			1.00	0.40±0.12	0.91±0.13	1.21±0.11	1.49±0.20
		1.50	2.00	0.27±0.08	0.77±0.13	1.05±0.10	1.20±0.17
			2.50	0.08±0.04	0.66±0.11	0.84±0.08	0.86±0.13
		2.50	3.00	±	0.90±0.13	0.90±0.09	0.97±0.13
			3.50	±	1.17±0.14	1.02±0.09	1.07±0.15
		3.50	4.00	±	1.05±0.15	1.12±0.08	1.09±0.12
			4.00	5.00	±	0.86±0.11	1.04±0.07
		5.00	6.50	±	±	0.73±0.05	0.83±0.07
			6.50	8.00	±	±	±
0.100	0.150	0.50	1.00	0.59±0.20	1.40±0.25	1.91±0.25	2.39±0.40
			1.00	0.87±0.20	0.87±0.15	1.17±0.13	1.56±0.22
		1.50	2.00	0.45±0.15	0.84±0.13	0.92±0.11	1.26±0.19
			2.50	0.39±0.10	0.77±0.15	0.70±0.08	0.59±0.11
		2.50	3.00	±	0.97±0.13	0.78±0.08	0.66±0.11
			3.00	3.50	±	0.87±0.12	0.67±0.07
		3.50	4.00	±	0.66±0.13	0.60±0.06	0.70±0.10
			4.00	5.00	±	0.59±0.10	0.55±0.05
		5.00	6.50	±	±	0.29±0.03	0.35±0.04
			6.50	8.00	±	±	±
0.150	0.200	0.50	1.00	0.93±0.30	1.52±0.28	1.55±0.23	1.83±0.34
			1.00	0.52±0.14	0.75±0.13	0.94±0.10	1.04±0.17
		1.50	2.00	0.21±0.09	0.63±0.11	0.65±0.08	0.79±0.15
			2.50	0.37±0.13	0.58±0.11	0.50±0.07	0.76±0.14
		2.50	3.00	±	0.42±0.08	0.43±0.06	0.48±0.09
			3.00	3.50	±	0.31±0.06	0.30±0.04
		3.50	4.00	±	0.33±0.06	0.22±0.03	0.40±0.07
			4.00	5.00	±	0.22±0.04	0.23±0.03
		5.00	6.50	±	±	0.058±0.013	0.13±0.03
			6.50	8.00	±	±	±
0.200	0.250	0.50	1.00	0.50±0.30	1.49±0.33	1.56±0.25	2.05±0.43
			1.00	0.30±0.14	0.84±0.18	0.89±0.15	0.89±0.22
		1.50	2.00	0.21±0.08	0.30±0.10	0.49±0.10	0.63±0.18
			2.50	0.13±0.06	0.30±0.09	0.37±0.08	0.41±0.14
		2.50	3.00	±	0.35±0.09	0.35±0.06	0.31±0.10
			3.00	3.50	±	0.20±0.06	0.19±0.04
		3.50	4.00	±	0.09±0.03	0.12±0.03	0.11±0.04
			4.00	5.00	±	0.10±0.03	0.11±0.03
		5.00	6.50	±	±	0.038±0.015	0.09±0.04
			6.50	8.00	±	±	±